

**UCSF**

**UC San Francisco Electronic Theses and Dissertations**

**Title**

Analysis of length control in short flagella mutants of *Chlamydomonas reinhardtii*

**Permalink**

<https://escholarship.org/uc/item/7h16z7ws>

**Author**

Kannegaard, Elisa Sandoval

**Publication Date**

2011

Peer reviewed|Thesis/dissertation

Analysis of length control in short flagella mutants of *Chlamydomonas reinhardtii*

by

Elisa Sandoval Kannegaard

DISSERTATION

Submitted in partial satisfaction of the requirements for the degree of

DOCTOR OF PHILOSOPHY

in

Cell Biology

in the

GRADUATE DIVISION

of the

UNIVERSITY OF CALIFORNIA, SAN FRANCISCO

Copyright (2011)  
by  
Elisa Sandoval Kannegaard

## ACKNOWLEDGEMENTS

First and foremost, I would like to thank Wallace for his great wealth of ideas and genuine enthusiasm for my work. I have always admired his excitement about science and his encyclopedic depth and breadth of knowledge, all of which give him a unique gift for especially creative metaphors. He is endlessly encouraging, an important and all too rare quality in an advisor, and I'm so glad to have had his support.

I also owe a debt of gratitude to the members of the Marshall lab. Our discussions were instrumental in focusing my thought processes and helping me direct the project. I am especially grateful to Kim Wemmer, Lani Keller, Will Ludington, Susanne Rafelski, and Juliette Azimzadeh for all their advice and support, both technical and emotional. I definitely couldn't have done this without their expertise and friendship.

I am fortunate to have the most loving, generous, and understanding family. My parents are amazing beyond words and have helped and inspired me in countless ways. My brother and his uncanny gift for music selection provided moments of great cheer and occasional catharsis during long hours at the microscope. Through it all, coming home to Kevin was the best part of every day.

Graduate school was a very long journey, and I had an amazing cast of characters with me each step of the way. To my family and friends— Sandovals, Kannegaards, Wooleys, the wine Friday ladies, the usual suspects, the yahoos, my fellow phoenixes— thank you for everything.



# Analysis of length control in short flagella mutants of *Chlamydomonas reinhardtii*

Elisa Sandoval Kannegaard

## ABSTRACT

How the complex spatial organization of a eukaryotic cell is achieved is an enduring and fundamental question in cell biology. The size and arrangement of organelles within the cell factor significantly in the establishment of cell architecture, yet little is known about how organelle size is controlled. This question is most easily addressed through study of linear structures, for which there is only one dimension that must be quantified. We have utilized the eukaryotic flagellum, a microtubule-based structure that protrudes outside the cell, as a model organelle to investigate the issue of organelle size control.

Eukaryotic flagella, alternatively known as cilia, are also known to be crucial for many developmental and physiological processes, yet their biogenesis, maintenance, and length control are not well understood. We have taken a genetic approach to understanding the system of flagellar length control in the unicellular green alga *Chlamydomonas reinhardtii*. *Chlamydomonas* cells possess two flagella, each typically 10-12µm in length, and this length is rigorously maintained. Whereas previous analyses of length control have concentrated upon long flagella (*lf*) mutants, we have thoroughly examined a novel collection of twenty short flagella (*shf*) mutants recovered from an insertional mutagenesis screen.

We have analyzed the flagellar length distributions, regeneration kinetics, and gene expression of these *shf* strains, and identified a class of mutants with defects in regeneration of the flagellar precursor pool. Of these precursor pool mutants, one appears to have a defect in flagellar gene induction during regeneration, and the others appear to have post-transcriptional defects. We have identified the molecular lesion of one of the strains with a post-transcriptional defect, and in doing so uncovered a previously unknown role for the microtubule-severing heterodimer katanin in flagellar length control.

## TABLE OF CONTENTS

### Chapter 1

Introduction.....	1
-------------------	---

### Chapter 2

Phenotype analysis of short flagella mutants.....	22
---	----

### Chapter 3

A role for katanin in flagellar length control.....	84
---	----

### Chapter 4

Summary & Perspective.....	117
----------------------------	-----

**LIST OF TABLES**

**Chapter 2**

Table 1.....82

Table 2.....83

**Chapter 3**

Table 1.....116

## LIST OF FIGURES

### Chapter 1

Figure 1.....	18
Figure 2.....	20

### Chapter 2

Figure 1.....	49
Figure 2.....	51
Figure 3.....	53
Figure 4.....	55
Figure 5.....	57
Figure 6.....	59
Figure 7.....	61
Figure 8.....	63
Figure 9.....	65
Figure 10.....	67
Figure 11.....	69
Figure 12.....	71
Figure 13.....	73
Figure 14.....	75
Figure 15.....	78

Figure 16.....80

**Chapter 3**

Figure 1.....106

Figure 2.....108

Figure 3.....110

Figure 4.....112

Figure 5.....114

# Chapter 1: Introduction

The complex spatial organization of a cell greatly impacts how that cell carries out its functions. In a eukaryotic cell, local concentrations of macromolecules in the cytoplasm as well as the geometry of organelles can influence intracellular biochemical reactions (Minton, 2006). How the cell achieves its intricate architecture is an enduring and fundamental question in cell biology. Indeed, understanding the mechanistic basis for cellular architecture was identified as a key outstanding question in biology for the new millennium (Shulman and St. Johnston, 1999; Kirschner, Gerhart, and Mitchison, 2000).

One crucial aspect of cellular architecture concerns organelles—the specification of their size, shape, number, and propagation (Rafelski and Marshall, 2008). In addition to their contribution to overall cell architecture, the structure and organization of individual organelles determines their ability to carry out their own specific biochemical or mechanical functions. Organelle size is a key parameter of organelle geometry and the size of any particular organelle can vary substantially from one cell type to another. This presumably reflects different functional requirements, as in pancreatic  $\beta$ -cells, which are characterized by a highly developed endoplasmic reticulum (ER) that provides capacity for the secretion of insulin. Similarly, it appears that the quantity of ER is actively regulated in response to the functional requirement for ER in protein folding, such that if excess unfolded protein accumulates, the ER is induced to expand (Bernales et al., 2006). In other cases, organelle size scales with cell size. For example, larger cells tend to form larger mitotic spindles (Wuehr et al., 2008). However, in no case are the detailed mechanisms that generate such scaling actually understood.



The problem of organelle size control is difficult to address experimentally because organelles typically have complex three-dimensional structures, which creates both technical problems in developing methodologies for measuring size and conceptual problems in deciding which parameters to use as indicators of size. For example, the ER forms an extensive network that ramifies throughout the cell. This makes it virtually impossible to visualize the ER tubules without going to the resolution level of the electron microscope, and also creates the difficulty of determining which aspect of the network to quantify as a measure of size. Is total surface area the relevant size, or is it the volume contained inside, or is it some other graph-theoretical property of the network? Due to such difficulties in size determination and analysis, the mechanisms controlling the size of most organelles remain almost completely unknown. In contrast to the challenges in measuring complicated three-dimensional organelles, the size control problem is far more easily addressed through study of linear structures, for which there is only one dimension that must be quantified.

### ***Length control in biological structures***

Study of length regulation in linear biological structures has yielded several paradigms for understanding the problem of size control (Marshall, 2004). Examples of such paradigms include quantal synthesis, in which overall size is determined by synthesizing a precise amount of a limiting precursor; dynamic balance, in which constant turnover ensures that steady state size is the result of an equilibrium between assembly and disassembly; and molecular ruler mechanisms in which the size of a structure

is determined by the size of another molecule or structure. The concept of a molecular ruler was first proposed 40 years ago (King, 1971) and has been shown to be a conserved mechanism for the regulation of tail length in several species of bacteriophage (Abuladze et al., 1994; Katsura, 1990; Pedersen et al., 2000). In bacteriophage, the ruler protein employs two domains: one that binds at the base of the tail, and one at the growing tip that inhibits binding of a growth-terminating molecule. When the tail lengthens past the ruler, the growth terminator can then bind the tail and prevent further growth. In phage lambda, the ruler protein is encoded by gene H. In-frame deletions in gene H give rise to abnormally short tails (Katsura and Hendrix, 1984), and engineered duplications in gene H cause longer tails (Katsura, 1987). Molecular rulers with slightly different mechanisms have also been proposed for length regulation of bacterial type III secretion needles and flagellar hooks (Journet et al., 2003; Shibata et al., 2007).

Whereas the structures discussed in the preceding paragraph consist of a mere handful of proteins, there are typically many more players in a eukaryotic organelle. For this reason, it is useful to examine size regulation in a more complex linear organelle such as the eukaryotic flagellum, alternately called a cilium (Figure 1). Not to be confused with the prokaryotic flagellum, which is a polymer of a single protein called flagellin, the eukaryotic flagellum is an intricate microtubule-based structure consisting of over 360 proteins (Pazour et al., 2005). Distinctions between eukaryotic flagella and cilia are historical; I shall use the terms interchangeably and refer to the structure by the name that is conventionally used in any particular context.

*Chlamydomonas reinhardtii*, a unicellular chlorophyte alga, has two flagella that are structurally and functionally homologous to vertebrate cilia (Figure 2).

*Chlamydomonas*, also known as green yeast, has long been used for studies of flagellar biology because it is amenable to classical genetic experiments, molecular biology techniques, and cellular manipulations. It is easily cultured in liquid or solid media, and phenotypic screens for flagellar defects are especially straightforward. Indeed some of the first mutants to be identified in *Chlamydomonas* had flagellar defects (Harris, 2001).

*Chlamydomonas* flagella are motile; they exhibit a breaststroke-like wave pattern that propels cells through the environment. In a wild type population, the flagella are 10-12  $\mu\text{m}$  in length. If one or both flagella are removed, they immediately begin to regenerate, and over the course of roughly two hours recover to the characteristic length of 10-12  $\mu\text{m}$ . These observations led to the hypothesis that *Chlamydomonas* cells control the length of their flagella.

### ***Evidence for a flagellar length control system***

One compelling line of evidence suggesting that a flagellar length control system exists is the fact that mutations have been found in which flagellar length distributions are altered. Genetic analysis of *Chlamydomonas* length-altering mutants has yielded a wealth of information about genes involved in flagellar length determination, including the *SHF* genes, whose mutants cause short flagella (Kuchka and Jarvik, 1987), and the *LF* genes, whose mutants cause both aflagellate cells and cells with atypically long flagella (Asleson and Lefebvre, 1998; Barsel et al., 1988; McVittie, 1972). However, the functions of these individual gene products are not known, nor are their interactions extensively

characterized, and to date there has been no clear mechanistic link between mutant phenotypes, model-based predictions of length control behavior, and the identities of molecular players. Similar evidence for length control of cilia and flagella arises from the fact that specific cilia-related diseases appear to involve alterations in ciliary length. Cilia play key roles in vertebrate development and disease (Marshall, 2008), and length defects are associated with a broad spectrum of pathology. Modulation of Notch signaling has been shown to affect the length of cilia in zebrafish, impacting the directionality and speed of fluid flow in Kupffer's vesicle, which plays a fundamental role in establishing left-right asymmetry of the developing embryo (Lopes et al., 2010). Additionally, excessively long cilia in photoreceptors are associated with progressive retinal degeneration in mice (Omori et al., 2010). Interestingly, a rat model of Meckel-Gruber syndrome exhibits tissue-specific length defects; cilia of the kidney collecting ducts are abnormally long, but sperm flagella are excessively short (Tammachote et al., 2009). Animal models for tuberous sclerosis complex (TSC) show increases in ciliary length, which appears to play a role in development of kidney cysts in this disease (DiBella et al., 2009). The fact that cilia length can be altered in specific genetic diseases further indicates that a length control system may exist, defects in which can contribute to pathology.

Another reason for thinking that a length control system exists arises from a comparison of flagellar length distributions to the length distributions of free microtubules. At its most fundamental, the flagellum is merely an ordered structure of microtubules, so one might imagine that the length of the flagellum is directly dictated by the dynamics of the underlying microtubules. The length distribution of microtubules

and microtubule structures has been predicted to be exponential (Dogterom and Leibler, 1993), thus, if there were no length control system present, one might predict that flagellar lengths would exhibit an exponential distribution with a large proportion of very short structures. Because *Chlamydomonas* flagella, which could theoretically be of any length, are typically 10-12 $\mu$ m, with a distribution that is clearly not exponential, it has been inferred that additional factors beyond simple microtubule dynamics must be at work to determine length. However, because the length distribution of an interconnected set of microtubules need not be the same as that of an individual microtubule, the non-exponential length distribution does not itself prove the existence of a length control system. In point of fact, there is not a strong theoretical basis by which one can look at a length distribution and determine a measure of how strongly it is regulated by active control. We can compare two length distributions and ask which is broader in order to compare the relative strengths of regulation, but this does not necessarily prove the existence of an active length control system.

In considering how an active control system might affect the distribution of flagellar lengths, the first order question is whether or not the length distribution is normal. The normal distribution, or Gaussian, is a good descriptor for complex phenomena arising from the additive effects of many random influences. The prevalence of normal distributions in biology arises from the central limit theorem, which guarantees that a sum of a sufficiently large number of independent random variables will have a normal distribution. For example, although size parameters of humans are the result of a multitude of genetic and environmental factors, chest measurements of Scottish soldiers

and heights of Swedish women have been shown to be normally distributed (Limpert, 2001). It is thus natural to ask whether the distribution of flagellar lengths deviates from a normal distribution. Two simple measures of deviation from normality are skewness and kurtosis. Skewness is a measure of the symmetry of the distribution relative to the mean, and is defined as the third central moment divided by the standard deviation cubed. A skewness of zero indicates a perfectly symmetrical distribution, which is characteristic of the normal distribution. Excess kurtosis is defined as the fourth central moment divided by the variance squared, minus 3, and is zero for a normal distribution. Deviations from a skewness or excess kurtosis of zero thus indicate departures from a normal distribution.

The distribution of flagellar lengths in a wild type population of *Chlamydomonas* has been reported to be leptokurtic, with a sharper peak around the mean than a normally distributed variable (Randall et al., 1969). This increased concentration of the distribution around the mean indicates that whatever system determines flagellar length, it is able to do so more precisely than a system that generates length from an additive combination of independent random processes. This does not directly prove the existence of an active length control system in and of itself, but does foment the idea that there must be a length control system that actively determines length. As will be discussed in Chapter 2, the distribution of lengths in an asynchronous population of cells can also be an indicator of the kinetics of flagellar elongation during the cell cycle.

### ***Flagellar assembly and the balance point model***

A key step in understanding flagellar morphogenesis was the discovery of intraflagellar transport (IFT), a bidirectional protein trafficking system that employs microtubule motors and adaptor proteins to move cargoes between the cell body and flagellar compartment as well as along the axoneme (Cole et al., 1998; Kozminski et al., 1993; Pazour et al., 1998). IFT is crucial for assembly and maintenance of the flagellum, which undergoes constant turnover of components at its distal tip (Johnson and Rosenbaum, 1992; Marshall and Rosenbaum, 2001). This constant turnover means that any length control system needs to ensure that the assembly and disassembly rates equal each other only at the desired length; when flagella are shorter than the target length, assembly must predominate, and when flagella are longer, disassembly must predominate. Thus the problem of flagellar length control becomes a problem of regulating assembly and disassembly rates as a function of length.

Appreciation of the dynamic nature of the flagellum and the observation that both the speed of IFT particle movement and the total quantity of IFT proteins in a flagellum is length-independent led to the formulation of the balance point model, which asserts that steady state length is determined by an equilibrium between assembly and disassembly (Engel et al., 2009; Marshall and Rosenbaum, 2001). Flagellar microtubules undergo constant disassembly at a rate which is independent of flagellar length (Marshall and Rosenbaum, 2001; Marshall et al., 2005), suggesting that whatever control system is acting to regulate length must do so by regulating assembly, rather than disassembly.

Furthermore, the fact that IFT is required for assembly indicates that control of IFT as a function of length would be one viable strategy to regulate flagellar length.

For a given IFT particle, the time it takes to deliver cargo at the distal tip and return to the cell body for another load of cargo is proportional to the length of the flagellum, therefore the frequency with which a single particle can deliver cargo is proportional to  $1/L$ . Since the total number of IFT particles is length-independent, the frequency of deliveries taking place at the tip will be proportional to  $N/L$ , where  $N$  is the number of particles and  $L$  is the length. Thus the rate at which tubulin, the main building block of the axoneme, can be brought to the tip will scale as  $1/L$ . Assuming the assembly rate at the tip depends on the rate of cargo delivery, there will therefore be only one value of the length for which the assembly rate equals the disassembly rate. For flagella that have become too long, the cargo delivery rate, and hence the assembly rate, scales as  $1/L$ , thus the assembly rate will drop below the disassembly rate and the flagellum will shorten. For short flagella, the assembly rate will exceed the disassembly rate and the flagellum will elongate. Thus, the steady-state solution is stable and the flagellum will tend to return to this length following any perturbation.

Modulation of length can affect flagellar function, and as such is likely subject to regulation. For example, the swimming speed of spermatozoa in a viscous fluid depends linearly on flagellar length (Dresdner and Katz, 1981), and may contribute to sperm selection and rates of fertilization (Holt et al., 2010). The motile cilia that line the respiratory tract provide another example of how ciliary length can impact function.



Mucociliary clearance, which continually cleanses the airways and is a vital defense against inhaled particulates and pathogens, has been predicted by mathematical models to depend on an interaction of mucus with the ciliary tips (Matsui et al., 1998). If cilia are too short, the tips cannot properly interact with the mucus to effectively move it through the airway. It has been shown that the impaired mucociliary clearance seen in cigarette smokers is a result of shortened cilia (Leopold et al., 2009). As the preceding examples demonstrate, although the optimal length varies depending on context, maintenance of the correct flagellar length is vital for proper function.

### ***Summary***

The work presented herein was conducted with the goal of identifying additional genes involved in flagellar length control, and to analyze the steady state flagellar length distributions of mutant strains in order to further develop mechanistic understanding of dynamic length control. Prior genetic analyses of length control have focused almost entirely on long flagella mutants, but we reasoned that for characterizing a control system, it does not make sense to focus solely on perturbations that increase the controlled quantity, and that perturbations that reduce the controlled quantity should be equally informative. Another reason to focus on short flagella mutants is that we felt they might reveal genes involved in promoting the synthesis of flagellar precursor proteins during assembly. Chapter 2 will describe my analysis of a novel collection of short flagella mutants of *Chlamydomonas* obtained in a screen for phototaxis defects, with a particular focus to determining which of these mutants are likely to affect precursor pool synthesis and mobilization. Several such genes were found in this study, one of which appears to

act at a transcriptional level and others that appear to act post-transcriptionally. Chapter 3 describes the cloning of one such gene that forms short flagella apparently due to a defect in precursor pool regeneration, and was found to encode the regulatory p80 subunit of the microtubule severing protein katanin. Collectively, this work significantly improves our understanding of short flagellar length mutants in *Chlamydomonas* as well as mechanisms underlying the regulation of organelle size.

## REFERENCES

- Abuladze, N.K., M. Gingery, J. Tsai, and F.A. Eiserling. 1994. Tail length determination in bacteriophage T4. *Virology*. 199:301-310.
- Asleson, C.M., and P.A. Lefebvre. 1998. Genetic analysis of flagellar length control in *Chlamydomonas reinhardtii*: a new long-flagella locus and extragenic suppressor mutations. *Genetics*. 148:693-702.
- Barsel, S.E., D.E. Wexler, and P.A. Lefebvre. 1988. Genetic analysis of long-flagella mutants of *Chlamydomonas reinhardtii*. *Genetics*. 118:637-648.
- Bernales, S., K.L. McDonald, and P. Walter. 2006. Autophagy counterbalances endoplasmic reticulum expansion during the unfolded protein response. *PLoS Biol.* 4:e423.
- Cole, D.G., D.R. Diener, A.L. Himelblau, P.L. Beech, J.C. Fuster, and J.L. Rosenbaum. 1998. *Chlamydomonas* kinesin-II-dependent intraflagellar transport (IFT): IFT particles contain proteins required for ciliary assembly in *Caenorhabditis elegans* sensory neurons. *J Cell Biol.* 141:993-1008.
- DiBella, L.M., A. Park, and Z. Sun. 2009. Zebrafish Tsc1 reveals functional interactions between the cilium and the TOR pathway. *Hum. Mol. Genet.* 18:595-606.
- Dogterom, M., and S. Leibler. 1993. Physical aspects of the growth and regulation of microtubule structures. *Phys Rev Lett.* 70:1347-1350.
- Dresdner, R.D., and D.F. Katz. 1981. Relationships of mammalian sperm motility and morphology to hydrodynamic aspects of cell function. *Biol Reprod.* 25:920-930.

- Engel, B.D., W.B. Ludington, and W.F. Marshall. 2009. Intraflagellar transport particle size scales inversely with flagellar length: revisiting the balance-point length control model. *J Cell Biol.* 187:81-89.
- Harris, E.H. 2001. Chlamydomonas as a Model Organism. *Annu Rev Plant Physiol Plant Mol Biol.* 52:363-406.
- Holt, W.V., M. Hernandez, L. Warrell, and N. Satake. 2010. The long and the short of sperm selection in vitro and in vivo: swim-up techniques select for the longer and faster swimming mammalian sperm. *J Evol Biol.* 23:598-608.
- Johnson, K.A., and J.L. Rosenbaum. 1992. Polarity of flagellar assembly in Chlamydomonas. *J Cell Biol.* 119:1605-1611.
- Journet, L., C. Agrain, P. Broz, and G.R. Cornelis. 2003. The needle length of bacterial injectisomes is determined by a molecular ruler. *Science.* 302:1757-1760.
- Katsura, I. 1987. Determination of bacteriophage lambda tail length by a protein ruler. *Nature.* 327:73-75.
- Katsura, I. 1990. Mechanism of length determination in bacteriophage lambda tails. *Adv Biophys.* 26:1-18.
- Katsura, I., and R.W. Hendrix. 1984. Length determination in bacteriophage lambda tails. *Cell.* 39:691-698.
- King, J. 1971. Bacteriophage T4 tail assembly: four steps in core formation. *J Mol Biol.* 58:693-709.
- Kirschner, M., J. Gerhart, and T. Mitchison. 2000. Molecular "vitalism". *Cell* 100:79-

- Kozminski, K.G., K.A. Johnson, P. Forscher, and J.L. Rosenbaum. 1993. A motility in the eukaryotic flagellum unrelated to flagellar beating. *Proc Natl Acad Sci U S A*. 90:5519-5523.
- Kuchka, M.R., and J.W. Jarvik. 1987. Short-Flagella Mutants of *Chlamydomonas reinhardtii*. *Genetics*. 115:685-691.
- Leopold, P.L., M.J. O'Mahony, X.J. Lian, A.E. Tilley, B.G. Harvey, and R.G. Crystal. 2009. Smoking is associated with shortened airway cilia. *PLoS ONE*. 4:e8157.
- Limpert, E., W.A. Stahel, and M. Abbt. 2001. Log-normal Distributions across the Sciences: Keys and Clues. *BioScience*. 51:341-352.
- Lopes, S.S., R. Lourenco, L. Pacheco, N. Moreno, J. Kreiling, and L. Saude. 2010. Notch signalling regulates left-right asymmetry through ciliary length control. *Development*. 137:3625-3632.
- Marshall, W.F., and J.L. Rosenbaum. 2001. Intraflagellar transport balances continuous turnover of outer doublet microtubules: implications for flagellar length control. *J Cell Biol*. 155:405-414.
- Marshall, W.F. 2004. Cellular length control systems. *Annu. Rev. Cell Dev. Biol*. 20:677-93.
- Marshall, W.F., H. Qin, M. Rodrigo-Brenni, and J.L. Rosenbaum. 2005. Flagellar length control system: testing a simple model based on intraflagellar transport and turnover. *Mol. Biol. Cell* 16:270-8.
- Marshall, W.F. 2008. The cell biological basis of ciliary disease. *J. Cell Biol*. 180:17-21.

- Matsui, H., S.H. Randell, S.W. Peretti, C.W. Davis, and R.C. Boucher. 1998. Coordinated clearance of periciliary liquid and mucus from airway surfaces. *J Clin Invest.* 102:1125-1131.
- McVittie, A. 1972. Flagellum mutants of *Chlamydomonas reinhardtii*. *J Gen Microbiol.* 71:525-540.
- Minton, A.P. 2006. How can biochemical reactions within cells differ from those in test tubes? *J Cell Sci.* 119:2863-2869.
- Omori, Y., T. Chaya, K. Katoh, N. Kajimura, S. Sato, K. Muraoka, S. Ueno, T. Koyasu, M. Kondo, and T. Furukawa. 2010. Negative regulation of ciliary length by ciliary male germ cell-associated kinase (Mak) is required for retinal photoreceptor survival. *Proc Natl Acad Sci U S A.* 107:22671-22676.
- Pazour, G.J., N. Agrin, J. Leszyk, and G.B. Witman. 2005. Proteomic analysis of a eukaryotic cilium. *J Cell Biol.* 170:103-113.
- Pazour, G.J., C.G. Wilkerson, and G.B. Witman. 1998. A dynein light chain is essential for the retrograde particle movement of intraflagellar transport (IFT). *J Cell Biol.* 141:979-992.
- Pedersen, M., S. Ostergaard, J. Bresciani, and F.K. Vogensen. 2000. Mutational analysis of two structural genes of the temperate lactococcal bacteriophage TP901-1 involved in tail length determination and baseplate assembly. *Virology.* 276:315-328.
- Rafelski, S.M., and W.F. Marshall. 2008. Building the cell: design principles of cellular architecture. *Nat Rev Mol Cell Biol.* 9:593-602.

- Randall, J., H.R. Munden, and P.H. Prest. 1969. The flagellar apparatus as a model organelle for the study of growth and morphopoiesis. With an appendix. Temperature control apparatus used in flagellar regeneration experiments. *Proc R Soc Lond B Biol Sci.* 173:31-62 passim.
- Shibata, S., N. Takahashi, F.F. Chevance, J.E. Karlinsey, K.T. Hughes, and S. Aizawa. 2007. FliK regulates flagellar hook length as an internal ruler. *Mol Microbiol.* 64:1404-1415.
- Shulman, J.M. and D. St. Johnston. 1999. Pattern formation in single cells. *Trends Cell Biol.* 9:M60-4.
- Tammachote, R., C.J. Hommerding, R.M. Sindors, C.A. Miller, P.G. Czarnecki, A.C. Leightner, J.L. Salisbury, C.J. Ward, V.E. Torres, V.H. Gattone, 2nd, and P.C. Harris. 2009. Ciliary and centrosomal defects associated with mutation and depletion of the Meckel syndrome genes MKS1 and MKS3. *Hum Mol Genet.* 18:3311-3323.

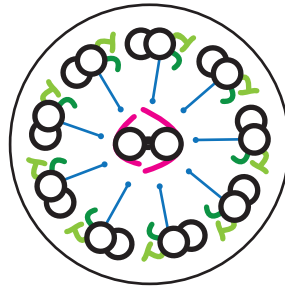
## FIGURES

### Figure 1. The eukaryotic flagellum

- (A) The transverse view of the flagellum shows the 9+2 structure of the axoneme, which refers to the nine outer doublet microtubules arrayed around two singlet microtubules called the central pair. The inner (dark green) and outer (light green) dynein arms generate motile force, and the radial spokes (blue) and central pair projections (magenta) regulate the motile machinery.
- (B) The longitudinal view of the flagellum shows two of the outer doublets, which are contiguous with the triplet microtubules of the centriole, and the central pair. Movement of proteins into the flagellar compartment and along its length is mediated by intraflagellar transport (IFT). Kinesin-2 is responsible for anterograde movement from the cell body to the distal tip, and cytoplasmic dynein 2 is responsible for retrograde movement. Even at steady state length, the distal tip undergoes constant turnover, requiring continual bidirectional protein trafficking.



**A**



**B**

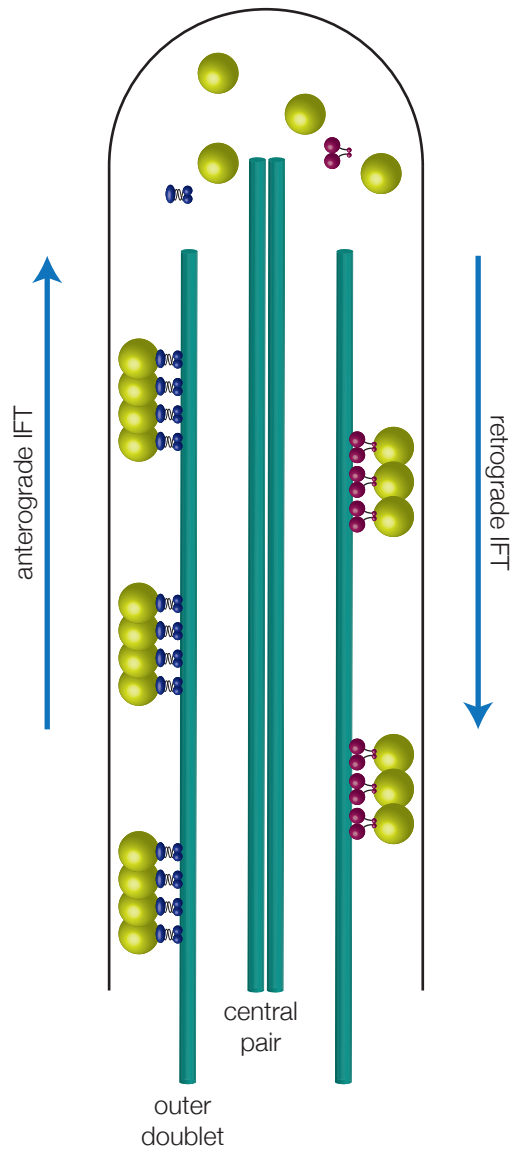
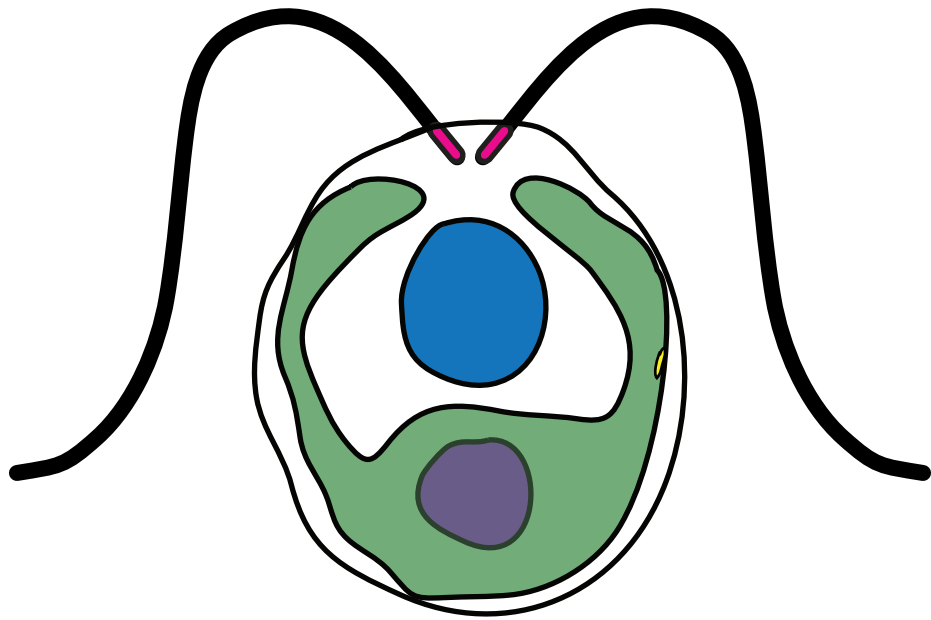


**Figure 2. *Chlamydomonas reinhardtii***

The *Chlamydomonas* cell is ovoid in shape, with a diameter of approximately 10µm. Two flagella, which originate in modified centrioles (magenta), protrude from the anterior end of the cell and are typically 10-12µm long. The nucleus (blue) is located centrally. A large cup-shaped chloroplast (green) fills much of the interior of the cell, and contains the pyrenoid (purple), which is the center of carbon fixation. The eyespot (yellow) is a light-sensing organelle located near the cell equator. The cell is enclosed by the plasma membrane and a rigid cell wall.



## Chapter 2: Phenotype analysis of short flagella mutants

## INTRODUCTION

Regulation of organelle size is a critical aspect of the determination of cell architecture, which in turn greatly impacts cell function (Chan and Marshall, 2010). The problem of organelle size control is most easily addressed through study of linear structures, for which there is only one dimension that must be quantified (Marshall, 2004). For this reason, the eukaryotic flagellum, a microtubule-based structure that protrudes outside the cell, is a classic model organelle.

One strategy for understanding the mechanism of flagellar length control has been analysis of mutations in the unicellular green alga *Chlamydomonas reinhardtii*. *Chlamydomonas* cells possess two flagella, each typically 10-12µm in length. This organism has long been a favored system for studies of flagellar biology due to its ease of culture and tractable yeast-like haploid genetics. Genetic analyses of *Chlamydomonas* have yielded a wealth of information about genes involved in flagellar length determination, including the identification of the *SHF* genes, whose mutants cause short flagella (Kuchka and Jarvik, 1987), and the *LF* genes, whose mutants cause both aflagellate cells and cells with atypically long flagella (Asleson and Lefebvre, 1998; Barsel et al., 1988; McVittie, 1972). Whereas much research has been done on the *lf* mutants, *shf* mutants have not been extensively studied. We therefore have set out to characterize a collection of novel *shf* mutants generated by insertional mutagenesis.

According to the balance point model of flagellar length control, steady state length is determined when rates of flagellar assembly and disassembly are equal (Marshall et al., 2005; Wemmer and Marshall, 2007). The disassembly rate is known to be constant, independent of length (Marshall and Rosenbaum, 2001). In contrast, assembly has been shown to be a length-dependent process; short flagella grow rapidly and long flagella grow more slowly. This is a consequence of the dependence of assembly on intraflagellar transport (IFT) and the fact that the number of IFT particles per flagellum is length-independent (Engel et al., 2009). Since each particle takes longer to deliver its cargo to the tip of longer flagella than to shorter flagella, the rate of transport per particle is inversely proportional to the length. For a fixed number of particles, the total transport rate is therefore inversely proportional to the length. The mechanisms that maintain the quantity of IFT particles constant per flagellum, independently of the flagellar length, remain unknown, but we would expect that genes controlling IFT particle quantity or function could be identified because they will affect the flagellar growth rate. The flagellar assembly rate is also dependent on the availability of a pool of precursor proteins in the cytoplasm. Prior studies have revealed the existence of such a pool but the molecular pathway that regulates the formation, maintenance, and regeneration of this pool is completely unknown. Again, we would expect that mutations affecting the pool maintenance pathway would alter flagellar growth kinetics as well as steady state length.

The time scale of flagellar assembly in wild type cells is on the order of 1 hour. By comparison, the typical doubling time for *Chlamydomonas* cells is about 8 hours. Thus, a change in assembly rate by merely a few fold would mean that flagellar assembly and the

cell cycle were operating on a comparable time scale. As a result, change in assembly rates may be expected to affect the observed distribution of lengths in a population of asynchronously dividing cells. One would expect that if the assembly rate were extremely slow, so that cells spend a long time reaching their final length, this would give rise to short flagella on average. In this case, even if the flagella can ultimately attain full length, the fact that they take so long to do so means that in an asynchronous culture, a substantial fraction of cells may have short flagella because they are still in the process of slowly assembling. Thus, in the case of an extreme reduction in assembly rate, we should see a frequency distribution of flagellar lengths that has a peak near wild type length but a skew towards shorter lengths. Searching for mutants with such a distribution is therefore suggested as a possible means to identify genes involved in regulating flagellar assembly. This methodology of inferring kinetics of growth from a distribution of lengths in an asynchronous population is formally equivalent to the ergodic rate analysis employed by Lahav et al. to deduce cell cycle progression rates from flow cytometry data (Tzur et al., 2009). For any given range of flagellar lengths, the faster the growth rate within that range, the fewer cells in the population that will have flagella of that length. This analysis requires the assumption that the quantity under measurement is a monotonic function of time, which is true for flagellar length. This method is far less time consuming than direct measurement of growth kinetics, facilitating analysis of a large number of mutants.

In addition to identifying mutants with alterations in flagellar growth kinetics, which would reveal genes involved in regulating growth rates, we were also interested in genes regulating production of flagellar precursor proteins. It has been well documented

that *Chlamydomonas* cells maintain a pool of proteins ready for incorporation into flagella, and therefore another possible cause of short flagella is that although the assembly machinery is normal, there is a defect in generating or maintaining the precursor pool. Previous studies established the existence of a precursor pool by showing that inhibition of protein synthesis during flagellar assembly causes cells to grow flagella of roughly half normal length (Lefebvre et al., 1978; Rosenbaum et al., 1969). In such cells the initial flagellar growth occurs with normal kinetics. In an asynchronous culture, because the cells are at all different stages of the cell cycle, the population will contain cells at all stages of the nonlinear flagellar assembly process, which at roughly two hours is far shorter than the average cell cycle of 8-10 hours. Because the initial growth phase is brief and occurs with rapid, normal kinetics, few cells in the population will have extremely short flagella. Likewise, if the regeneration of the precursor pool is defective, few cells will reach full length. Because precursor regeneration is presumed to take place gradually over a long period of time, most of interphase will be spent during the slow phase of flagellar assembly, when the pool is depleted. In this scenario, the length distribution will be dominated by intermediate length flagella, giving rise to a platykurtic, or flat, length distribution.

It is also certainly possible that short flagella may arise from defects having nothing to do with dynamic size control. For example, a mutation in a protein integral to the axoneme would weaken the overall structure, leading to a higher rate of disassembly at steady state. In this case, because the assembly rate is inversely proportional to the length, the flagellum would equilibrate at a new shorter length. Thus mutations in



important axonemal structure proteins would be predicted to result in short average length. However, since the dependence of assembly rate on length would not be affected, the length distribution should still be tightly focused around the mean just as in wild-type cells, resulting in a short average length without a substantial increase in the standard deviation.

The foregoing considerations suggest that we should expect to see three classes of mutations, all of which may have short average length. Mutations with defects in regulating IFT or pool regeneration are expected to have an average length near wild type but with a strong negative skew, reflecting the population of cells in an asynchronous population that have not yet reached their steady state length due to reduced rate of flagellar growth. Mutations with defects in the length control system itself would be expected to show a greatly increased variance in length and possibly a less peaked distribution. Finally, mutations with axonemal structural defects would be expected to show a reduced average length but without a large increase in variance.

In order to investigate what factors influence the determination of length, and in particular to identify genes involved in regenerating the flagellar precursor protein pool, we have analyzed a set of novel *shf* mutants using a combination of statistical analysis of length distributions, direct measurement of flagellar regeneration kinetics, quantitative analysis of flagellar precursor protein-encoding gene expression levels, and measurement of precursor pool regeneration kinetics. This combined analysis has allowed us to identify five strains with defects in flagellar precursor pool generation, including one strain

deficient in flagellar gene regulation. These represent, to our knowledge, the first known mutants with specific defects in precursor pool regeneration, and their identification validates our original plan of using the *shf* mutant phenotype as a primary screening method.

## RESULTS

### Characterization of wild type strain and established mutants

Because flagellar length is sensitive to growth conditions, we first determined that our culture conditions were ideal for maintenance of steady state flagellar lengths consistent with published values of mean length of 10-12 $\mu$ m and standard deviation of 1.8 (Randall et al., 1969). The wild type flagellar length distribution is leptokurtic with insignificant skew; the distribution has a sharp peak at the mean and symmetric tails (Figure 1).

Although numerous flagellar mutants have been isolated and characterized, a thorough examination of flagellar length distribution in these mutants has been lacking. Because there is a relationship between flagellar length and swimming ability in *Chlamydomonas*, we examined mutants with paralyzed flagella (*pf*) in addition to the canonical *shf* mutants. Many *pf* strains have been reported to have flagella of wild type length, so we analyzed six *pf* mutants with different underlying defects: the radial spoke-deficient strains *pf14* and *pf26*, and the central pair deficient strains *pf15*, *pf18*, *pf19*, and *pf20*. While it is true that some the *pf* strains have a subset of cells with wild type length flagella, analysis of the full populations indicates that in addition to motility defects, these cells also exhibit a length control defect (Figure 2). The length defects of the *shf* strains had been described previously, but no analysis of length distributions had been presented to date. We obtained the classical *shf* strains *shf1-253*, *shf2-1284*, and *shf3-1851*, however the latter two strains seem to have changed phenotypes since they were first isolated, a

phenomenon which has been noted to occur in *Chlamydomonas*. *Shf2-1284* cells were predominantly flagella-less, typically referred to as bald (*bld*), and *shf3-1851* cells possessed flagella of near wild type length. *Shf1-253* cells exhibited the expected phenotype, with a mean flagellar length of 5.15 $\mu$ m.

### **Classification of novel length control mutants**

We then measured flagellar lengths for twenty insertional mutant strains that had been characterized as being defective in phototaxis and visually noted as having short flagella (Figure 4, Feldman et al., 2007). Strains with flagella of unequal length or variable numbers of flagella were excluded from the cohort to be examined. Of the twenty insertional mutant strains, eighteen had mean lengths significantly different than the wild type strain (Table 1). The two remaining strains, mutants 9111 and 7107, were included in further analysis because although their mean length was not significantly different from wild type, a subset of cells did have atypically short flagella, a phenotype that is not observed in the wild type strain.

As discussed in the introduction, the fact that the time scales of flagellar assembly and the cell cycle are both of a similar order of magnitude (hours) suggested that mutations that reduced the flagellar growth rate would produce a negative skew. Such mutations would be of great interest to us as they might reveal components of the flagellar assembly or transport machinery. Furthermore, since one manifestation of the length control system is the restriction of length variation, resulting in a distribution that is highly peaked at the mean, we would expect *a priori* that mutations that simply shift the

set-point of the system would maintain this peaked form of the distribution but just alter the value of the mean, while mutations that broke the control system itself should produce a broader, less peaked distribution.

Based on these considerations, we set out to classify short flagella mutants into groups that might have distinct effects on the length control system. We utilized descriptive statistics of the flagellar length distributions to categorize the insertional mutant strains (Table 1). Examination of the skew and kurtosis of the distributions allowed us to strictly define three categories: Class I (positive kurtosis, positive skew), Class II (positive kurtosis, negative skew), and Class III (negative kurtosis, variable skew). We expect that these differences in distribution characteristics could reflect differences in growth kinetics based on the fact that for an asynchronous population of identical cells whose flagella increase in length as a monotonic function of time, the fraction of cells with lengths in an given small length range will be inversely proportional to the rate of growth at that length. This assertion assumes ergodicity: that time-averaged behavior for individual cells matches cell-averaged behavior for the whole population. If there is more than one distinct subtype of cells in the population, the assumption of ergodicity would be false and the analysis would not be applicable. However, our initial analysis is merely a secondary screen used to classify potentially interesting candidates to further examine by direct means, allowing us to disregard this concern.

Using this analysis, we found that Class I comprises seven mutants with significant positive kurtosis and significant positive skew (Table 1, Figure 5). Strains in

this category have an extreme length defect, with flagella of mean length less than  $4\mu\text{m}$ . Six of the seven strains exhibited a range of lengths in excess of  $4\mu\text{m}$ , with mutant 802 exhibiting the widest range,  $.96\mu\text{m}$ - $11.46\mu\text{m}$ . This type of length distribution in which average length is reduced but kurtosis remains positive is what we expect from mutants having defects in axonemal integrity, although that need not be the only possible explanation.

Class II comprises eight strains with negative skew and positive kurtosis. Class II mutants have mean lengths of  $9$ - $10.5\mu\text{m}$ , approaching the wild type mean length. Indeed, the mean flagellar length of Class II mutants 9111 and 7107 does not differ significantly from the wild type mean length. The main features distinguishing Class II mutants from the wild type strain are the range of flagellar lengths and the skew of the distributions (Figure 6). Whereas the mean lengths fall between  $9$  and  $10.5\mu\text{m}$ , and maximal lengths between  $13$  and  $17\mu\text{m}$ , similar to the wild type mean of  $\sim 11\mu\text{m}$  and maximum of  $\sim 15\mu\text{m}$ , the wild type distribution minimum is  $8.79\mu\text{m}$  and Class II minima range from a mere  $.63\mu\text{m}$  to  $6.12\mu\text{m}$ . This type of length distribution is consistent with a reduced rate of flagellar elongation, such that flagella take longer to reach their final length. Slower elongation results in a reduced mean length and negative skew, but because the length control system itself is still operating, a large fraction of cells possess flagella of appropriate length, giving rise to positive kurtosis.

In contrast to the other two classes, which are marked by length distributions with positive kurtosis, characterizing a distribution tightly peaked around the mean, all strains

in Class III showed length distributions that were platykurtic, with significant negative kurtosis (Figure 7). Class III mutants have intermediate mean lengths, 4-7 $\mu$ m, as well as an extremely broad range of lengths manifest as high standard deviation. These strains are thus qualitatively different from Class I and Class II because they have lost the characteristic tight distribution of lengths seen in wild type cells, the canonical *shf* mutants, and our other two classes of insertional *shf* mutants. As previously discussed, this type of distribution is consistent with our expectations for mutations affecting synthesis of the flagellar precursor pool.

It is interesting to note that our classification revealed a correlation between length and variability. Within the Class II mutants, which have length distributions most similar to wild type, the strains with shorter average length had larger standard deviations in length, and as mean length approaches the wild type value, the standard deviation decreases (Figure 8A). In order to analyze variability in all strains, the coefficient of variation (CV) is a more useful metric because the mean flagellar lengths in our study vary by nearly two orders of magnitude. We found a statistically significant ( $p < .0001$ ) negative correlation between mean length and CV on a strain-by-strain basis (Figure 8B).

### **Assembly kinetics of *shf* mutants**

Having identified candidate mutants whose length distributions suggested a possible alteration of growth kinetics, we sought to directly measure flagellar growth kinetics. Because the flagellum is a dynamic organelle, its steady state length depends directly on its assembly rate, as stated in the balance point model. Postulating that a

defect in flagellar assembly was responsible for causing the length defect in one or more *shf* mutants, we took advantage of the fact that *Chlamydomonas* cells can be induced by pH shock to shed and regrow their flagella, allowing us to observe flagellar growth kinetics uncoupled from the cell cycle.

The regeneration of wild type flagella proceeds in phases, beginning with a rapid growth phase lasting approximately 40 minutes, followed by slower growth for approximately 80 minutes, when flagella have regained roughly 90% of their initial length (Figure 10A). The final slow elongation phase to pre-shock length can last up to 8 hours (Rosenbaum et al., 1969). The length distribution achieved after 120 minutes of regeneration is similar to the initial distribution (Figure 9).

In Class II mutants, flagellar regeneration took place with similar kinetics to the wild type strain, with an initial rapid growth phase followed by decelerating growth (Figure 10C, Table 2). Because the flagella of Class I mutants are predominantly very short, it was not possible to observe their regeneration kinetics, excepting the two Class I mutants with greatest steady state mean length, mutant 267 and mutant 802. Whereas the regeneration of mutant 802 flagella did not proceed in the canonical phases, the regeneration kinetics of mutant 267 flagella did show the initial rapid growth phase, only to have a decrease in mean length after 40 minutes (Figure 10B). This intriguing result suggests that there may be an active shortening process causing strain 267 to have short flagella.



The flagellar regeneration kinetics of Class III mutants are shown in Figure 11. In Class III mutants, initial growth is more rapid than later growth, however the initial growth rate is slower than that of the wild type strain and of Class II mutants (Table 2). When wild type flagella regenerate in the absence of protein synthesis, they initially regenerate at the same rate as cells with active protein synthesis (Rosenbaum et al., 1969). However, after the initial rapid growth phase, growth ceases and flagella only reach about half of their typical steady state length (Figure 11A). In Class III mutants, the regeneration curves plateau abruptly at a short length relative to wild type, and in this sense are reminiscent of wild type cells treated with the protein synthesis inhibitor cycloheximide. This might be the expected result for a mutant with defects in precursor pool regeneration. However, in contrast to cycloheximide-treated wild type cells, the initial growth rate is slightly reduced. This could indicate some pool-independent effect of the mutation, or it could indicate that mutants have a reduced pool relative to wild type cells at the outset of the time course.

### **Assessment of the flagellar precursor pool in Class III mutants**

Based on the facts that Class III mutants exhibited flagellar length distributions predicted to result from defects pertaining to the precursor pool, and their regeneration kinetics mimicked those of wild type flagella forced to assemble in the absence of protein synthesis, we hypothesized that Class III mutants have a smaller than normal precursor pool or impaired regeneration of the precursor pool. We estimated the size of the functional flagellar precursor pool by using cycloheximide to prevent protein synthesis during flagellar assembly, such that the axoneme must be completely built from existing

precursors, and measured the final length attained. The Class III mutants 784, 4580, 1464, and 3584 all regenerated significantly shorter flagella than the wild type strain under these conditions (Figure 12). However, it is possible that these strains do not fully regenerate their flagella for reasons not pertaining to the precursor pool, or that the underlying cause of their *shf* phenotype also prevents their full regeneration. For this reason, we wished to examine dynamic changes in the precursor pool during flagellar regeneration more directly.

The kinetics with which the precursor pool regenerates during flagellar assembly can be directly assessed using a method developed by Lefebvre and Rosenbaum (Lefebvre, 1978), which entails performing dual deflagellations in the presence of cycloheximide. In this procedure, flagella are detached by pH shock and allowed to regenerate. Actively regenerating flagella are subjected to an additional pH shock in the presence of cycloheximide at a series of set time intervals then allowed to fully regenerate after the second shock. Because regeneration during the second shock depends on whatever precursor pool was present before the second shock was initiated (since protein synthesis was inhibited at the same time that the second shock was performed), a plot of the final length versus the time at which the second shock was performed yields a plot of the effective pool size as a function of time. Analysis of pool dynamics using this dual shock assay in wild type cells has shown that the pool of flagellar precursors is depleted during the first 40 minutes of regeneration, then begins to accumulate again (Lefebvre et al., 1978).

When we applied this dual-shock measurement method to our mutants, we found that each of the Class III mutants also showed pool depletion by  $t=40$  minutes, just as was seen in wild type, however the extent of pool recovery varied from strain to strain (Figure 13). In mutants 784 and 4580, the pool did recover somewhat, albeit slowly and incompletely. Pool recovery was not evident in mutants 1464 and 3584. Thus, all four Class III mutants tested showed a clear effect on the regeneration of the effective precursor pool in comparison to wild type cells. We emphasize that this measurement is not a direct measurement of any particular protein component of the flagellum, but rather a measurement of the effective pool size in terms of the flagellar length that can be grown with a particular quantity of precursor.

### **Gene induction during flagellar assembly**

Given our results above, it appears that the Class III mutants have a defect in regeneration of the flagellar precursor pool. The precursor pool is known to be under transcriptional control, such that during the process of regeneration, expression of flagellar genes is dramatically upregulated (Lefebvre and Rosenbaum, 1986; Stolc et al., 2005). Because a failure to induce flagellar gene expression would certainly prevent regeneration of a precursor pool, one obvious reason for the failure to regenerate the pool in the Class III mutants would be that perhaps the genes defective in these mutants are part of the pathway controlling transcription of flagellar protein-specific genes. Currently none of the components of this pathway are known, so we were extremely interested in determining whether the Class III mutants might reveal genes that regulate flagellar

precursor protein-encoding genes. To do this, we tested whether *shf* mutants were capable of proper gene induction utilizing quantitative RT-PCR.

We tested the induction of the genes for  $\alpha$ -tubulin (*TUA1*), radial spoke protein 3 (*RSP3*), and radial spoke protein 6 (*RSP6*), all of which have previously been shown to be strongly upregulated during flagellar regeneration (Stolc et al., 2005). Of those three genes, *RSP3* showed the most robust and reproducible induction in wild type cells (Figure 14), and was therefore selected as the representative gene for assaying the mutant collection. The *RBCS2B* gene, which encodes a subunit of the abundant photosynthesis enzyme ribulose-1,5-bisphosphate carboxylase oxygenase, commonly known as RuBisCo, was selected as the control "housekeeping" gene for normalizing expression levels.

We then examined transcriptional induction in our collection of mutants as well as selected other *shf* and *pf* mutants, expecting to find a defect in Class III mutants, which showed a defect in pool regeneration as assessed in Figure 13. Because peak induction of most flagellar genes occurs 30 minutes after deflagellation (Stolc et al., 2005), we selected this time point for comparison of induction across strains. Interestingly, induction was variable among the cohort examined (Figure 15). The *shf3* strain and mutants 802 and 7107 had significantly higher *RSP3* expression than the wild type strain, and the strains *pf18*, *shf1*, and mutants 784, 5836, 5840, and 6773 had significantly lower expression than the wild type strain. Of these low inducers, all but strain 784 were found to have significant numbers of *bld* cells, suggesting that the presence of a flagellum is necessary to induce expression of flagellar genes following pH shock.

Surprisingly, of the Class III mutants, only mutant 784 showed decreased induction of *RSP3*. In three of the four Class III mutants with partial or complete loss of pool regeneration (mutants 1464, 3584, and 4580), we found that expression of *RSP3* was induced at levels similar to wild type (Figures 15, 16). However, the kinetics of expression were different; these three strains had significantly higher expression than the wild type strain at 45 minutes post-deflagellation, although expression levels equalized by the 60 minute time point. We therefore suspect that in these mutants the primary defect caused by the mutation is lack of flagellar assembly, and then the failure to induce flagellar genes is a secondary consequence.

## DISCUSSION

The results presented here are, to our knowledge, the first demonstration of mutants that alter the regeneration of the flagellar precursor pool. The fact that such mutants were recovered in a screen of short flagella mutants confirms the importance of precursor pool regulation for the dynamic control of flagellar length. It is particularly interesting to note that the Class III mutants described here, all of which show a defect in precursor pool regeneration, share a similar distribution of flagellar lengths suggestive of a broken system rather than a shift in the set point as was seen in Class I and II mutants.

Measurement systems are typically described in terms of accuracy and precision, with accuracy referring to how close a measured quantity is to the true value, and precision referring to the degree to which repeated measurements of the same quantity vary. If a measurement is subject to many small sources of random error and negligible systematic error, the measured values will be distributed in accordance with a bell-shaped curve centered on the true value (Taylor, 1996).

If we are to consider flagellar length control as a measurement system, we can think of this system acting at the population level, with each cell representing a reproduction of the measurement. There is no single true value for flagellar length; it can vary in response to cellular context, fluid flow conditions, and various other parameters. Here, we consider the mean flagellar length of wild type flagella to be the reference value for assessment of accuracy, and the precision of the system is reflected in the distribution

of flagellar lengths in the population. Additionally, application of the descriptive statistics skew and kurtosis and their implications leads us to propose hypotheses about length control mechanism and function; skew indicates systematic error, and kurtosis that variance is the result of rare extreme deviations rather than frequent modest deviations.

All length control mutants in our collection have defects in accuracy or both accuracy and precision, as evidenced by the wide ranges of lengths observed and skewed distributions. These skewed distributions imply systematic errors in the flagellar measurement system. It is intriguing to note that in our collection of *shf* mutants, we obtained strains with leptokurtic flagellar length distributions at either end of our observed range of lengths, but not mutants with leptokurtic distributions centered at an intermediate length between 3 and 8  $\mu\text{m}$ . This suggests that length control is a complex system with many components, rather than being controlled by a “length sensor” that determines a length set point, as has been previously proposed (Tam et al., 2007).

The balance point model asserts that steady state flagellar length is achieved when the flagellar assembly rate and disassembly rate are equal. The model predicts that if the assembly rate is slowed or the disassembly rate enhanced, a cell may possess short flagella. Given that data has shown that the disassembly rate is constant, it is perhaps unsurprising that our length control mutants appear to have defects in the flagellar assembly rate.

We have shown that the initial assembly rate of Class I and Class III mutants is slower than wild type and Class II mutants. Future experiments will address whether this

slower growth rate is due to a change in IFT motor speeds, although it is technically challenging to observe IFT in short flagella.

When new protein synthesis is inhibited by the addition of cycloheximide during flagellar regeneration, all short flagella mutants attain a final length shorter than that of wild type in cycloheximide, and much shorter than their regenerated length without cycloheximide. This implies that protein synthesis may play a role in causing the *shf* phenotype, but there are other complicating factors at play as well.

Each of the Class III mutant strains is capable of growing full-length flagella, but only a small percentage of cells in the population do so. Given this heterogeneity, it would be interesting to compare and contrast the results of single cell regeneration experiments conducted on cells within a single strain to address the question of cellular memory. Do the conditions in the cell reproduce the same length flagella repeatedly in a single cell, or are there strains in which length determination is a stochastic process?

Our identification of mutants that block or slow pool regeneration give us a new set of tools to further probe the relation of precursor synthesis and length control, and will serve as the basis for future experiments. These phenotypes also raise the question of what proteins are encoded by the effective genes. We will take up this question in Chapter 3, in which we describe the cloning of one of the class III mutants described here.



## EXPERIMENTAL PROCEDURES

### *Strains & culture*

*Chlamydomonas reinhardtii* cells were maintained on TAP plates (Harris, 1989) and experimental cultures were grown in M1 minimal media (Harris, 1989). Insertional mutants were obtained from Jessica Feldman (Feldman et al., 2007) and additional strains were obtained from the *Chlamydomonas* Genetics Center. Cells were cultured at 21°C with constant light and in a rotating roller drum to provide aeration.

### *Length measurements*

Cells were fixed in 1% glutaraldehyde in PBS and imaged using differential interference contrast (DIC) optics with a 60x objective on a Deltavision microscope (Applied Precision). Measurements were obtained by hand tracing flagella using Softworx software (Applied Precision). Only cells with two visible, measurable flagella were included in the analysis.

### *Analysis of length distributions*

Length measurement data were analyzed using Microsoft Excel to calculate skew and excess kurtosis values. Skew was determined to be significant if the skew value was greater than twice the standard error of skew, defined as  $\sqrt{6/N}$ . Kurtosis was determined to be significant if the excess kurtosis value was greater than twice the standard error of kurtosis, defined as  $\sqrt{24/N}$ .

### ***Deflagellation by pH shock***

Cells were spun down at 1500 x g for 2 minutes in a bench top centrifuge and resuspended in M1 medium acidified to pH 4.5 with acetic acid. After a 1-minute incubation in acidic M1, cells were centrifuged again, supernatant was decanted, and cells were resuspended in fresh neutral M1 medium.

### ***Flagellar regeneration assay***

Cells were subjected to acidic pH shock as described above. Resuspended cells in neutral M1 medium were incubated at 21°C with constant light in a rotating roller drum. Aliquots of cells were withdrawn at 10-minute intervals and mixed with an equal volume of 2% glutaraldehyde in 1x PBS to fix. Length measurements were performed as described above.

### ***Calculation of flagellar growth rate***

Measurements obtained in flagellar regeneration assays were plotted using GraphPad Prism software. The values from the 10, 20, 30, and 40-minute time points were used to generate a linear regression, the slope of which gives the growth per minute.

### ***Quantitative RT-PCR***

To measure gene expression during flagellar assembly, total RNA was isolated from *Chlamydomonas* cells prior to deflagellation and at 30, 45, and 60 minutes after deflagellation as previously described (Stolc et al., 2005) with an additional purification

step using a PureLink RNA mini kit (Invitrogen). RNA was reverse transcribed using the SuperScript VILO kit (Invitrogen), with 1 µg of total RNA per reaction. cDNA was diluted 1:20 and used for quantitative PCR with Taq and SYBR Green and analyzed with a DNA Engine Opticon system (MJ Research). C<sub>T</sub> values were obtained using Opticon software (MJ Research).

### ***Flagellar precursor pool estimation***

Cells were subjected to deflagellation by pH shock as described above. At 10-minute intervals following the initial shock, cells were subjected to a second shock with cycloheximide at 10 µg/ml final concentration in both the acidic shock medium and neutral recovery medium. Cells were permitted to recover from the second shock for two hours before fixation and flagellar length measurements were performed as described above.

### ***Statistical analysis***

Statistical tests were performed using GraphPad Prism software.

## REFERENCES

- Asleson, C.M., and P.A. Lefebvre. 1998. Genetic analysis of flagellar length control in *Chlamydomonas reinhardtii*: a new long-flagella locus and extragenic suppressor mutations. *Genetics*. 148:693-702.
- Barsel, S.E., D.E. Wexler, and P.A. Lefebvre. 1988. Genetic analysis of long-flagella mutants of *Chlamydomonas reinhardtii*. *Genetics*. 118:637-648.
- Chan, Y.H., and W.F. Marshall. 2010. Scaling properties of cell and organelle size. *Organogenesis*. 6:88-96.
- Engel, B.D., W.B. Ludington, and W.F. Marshall. 2009. Intraflagellar transport particle size scales inversely with flagellar length: revisiting the balance-point length control model. *J Cell Biol*. 187:81-89.
- Feldman, J.L., S. Geimer, and W.F. Marshall. 2007. The mother centriole plays an instructive role in defining cell geometry. *PLoS Biol*. 5:e149.
- Kuchka, M.R., and J.W. Jarvik. 1987. Short-Flagella Mutants of *Chlamydomonas reinhardtii*. *Genetics*. 115:685-691.
- Lefebvre, P.A., S.A. Nordstrom, J.E. Moulder, and J.L. Rosenbaum. 1978. Flagellar elongation and shortening in *Chlamydomonas*. IV. Effects of flagellar detachment, regeneration, and resorption on the induction of flagellar protein synthesis. *J Cell Biol*. 78:8-27.
- Lefebvre, P.A., and J.L. Rosenbaum. 1986. Regulation of the synthesis and assembly of ciliary and flagellar proteins during regeneration. *Annu Rev Cell Biol*. 2:517-546.
- Marshall, W.F. 2004. Cellular length control systems. *Annu Rev Cell Dev Biol*. 20:677-693.

- Marshall, W.F., H. Qin, M. Rodrigo Brenni, and J.L. Rosenbaum. 2005. Flagellar length control system: testing a simple model based on intraflagellar transport and turnover. *Mol Biol Cell*. 16:270-278.
- Marshall, W.F., and J.L. Rosenbaum. 2001. Intraflagellar transport balances continuous turnover of outer doublet microtubules: implications for flagellar length control. *J Cell Biol*. 155:405-414.
- McVittie, A. 1972. Flagellum mutants of *Chlamydomonas reinhardtii*. *J Gen Microbiol*. 71:525-540.
- Randall, J., H.R. Munden, and P.H. Prest. 1969. The flagellar apparatus as a model organelle for the study of growth and morphopoiesis. With an appendix. Temperature control apparatus used in flagellar regeneration experiments. *Proc R Soc Lond B Biol Sci*. 173:31-62 passim.
- Rosenbaum, J.L., J.E. Moulder, and D.L. Ringo. 1969. Flagellar elongation and shortening in *Chlamydomonas*. The use of cycloheximide and colchicine to study the synthesis and assembly of flagellar proteins. *J Cell Biol*. 41:600-619.
- Stolc, V., M.P. Samanta, W. Tongprasit, and W.F. Marshall. 2005. Genome-wide transcriptional analysis of flagellar regeneration in *Chlamydomonas reinhardtii* identifies orthologs of ciliary disease genes. *Proc Natl Acad Sci U S A*. 102:3703-3707.
- Tam, L.W., N.F. Wilson, and P.A. Lefebvre. 2007. A CDK-related kinase regulates the length and assembly of flagella in *Chlamydomonas*. *J Cell Biol*. 176:819-829.
- Taylor, J.R. 1996. An Introduction to Error Analysis: The Study of Uncertainties in Physical Measurements. University Science Books.

- Tzur, A., R. Kafri, V.S. LeBleu, G. Lahav, and M.W. Kirschner. 2009. Cell growth and size homeostasis in proliferating animal cells. *Science*. 325:167-171.
- Wemmer, K.A., and W.F. Marshall. 2007. Flagellar length control in *Chlamydomonas*-- paradigm for organelle size regulation. *Int Rev Cytol*. 260:175-212.

## FIGURES & TABLES

### **Figure 1. Flagellar length distribution of wild type strain**

Cells were fixed in glutaraldehyde prior to visualization and measurement of flagella.

Flagellar length is expressed as mean  $\pm$  standard error of the mean. Wild type strain cc-125 flagellar length=  $11.03 \pm .09\mu\text{m}$ , skew= .06, kurtosis= .43. N= 166 flagella from three different experimental cultures.

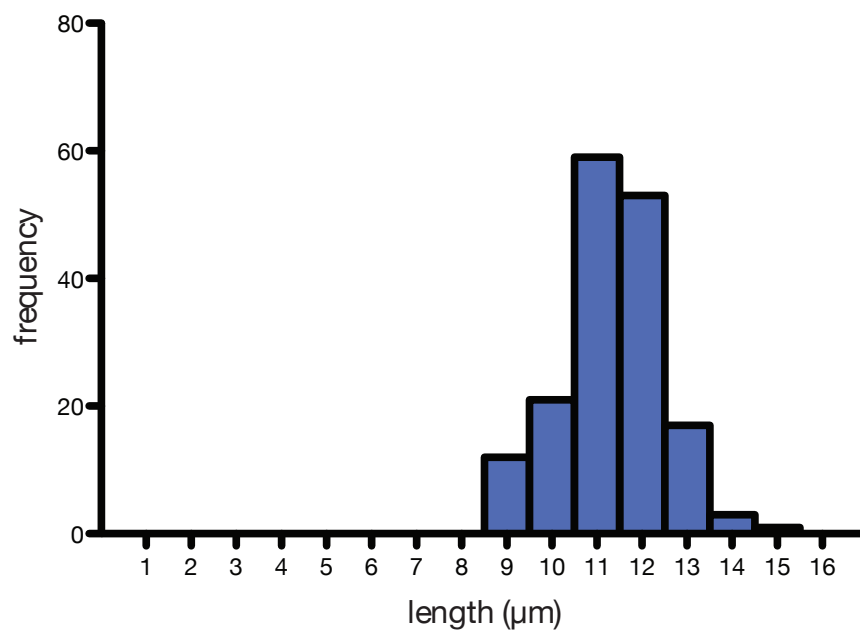




**Figure 2. Flagellar length distributions of *pf* mutants**

Cells were fixed in glutaraldehyde prior to visualization and measurement of flagella.

Flagellar length is expressed as mean  $\pm$  standard error of the mean.

(A) *pf14* flagellar length=  $2.82 \pm .37\mu\text{m}$ , skew= 1.02, kurtosis= 1.23 (N= 21 flagella)

(B) *pf15* flagellar length=  $6.11 \pm .28\mu\text{m}$ , skew= .61, kurtosis= -.66 (N= 153 flagella)

(C) *pf18* flagellar length=  $4.19 \pm .38\mu\text{m}$ , skew= 1.53, kurtosis= 1.37 (N= 62 flagella)

(D) *pf19* flagellar length=  $1.92 \pm .11\mu\text{m}$ , skew= 1.07, kurtosis= .14 (N= 90 flagella)

(E) *pf20* flagellar length=  $6.07 \pm .58\mu\text{m}$ , skew= .34, kurtosis= -1.48 (N= 54 flagella)

(F) *pf26* flagellar length=  $11.71 \pm .76\mu\text{m}$ , skew= 1.71, kurtosis= 2.21 (N= 20 flagella)

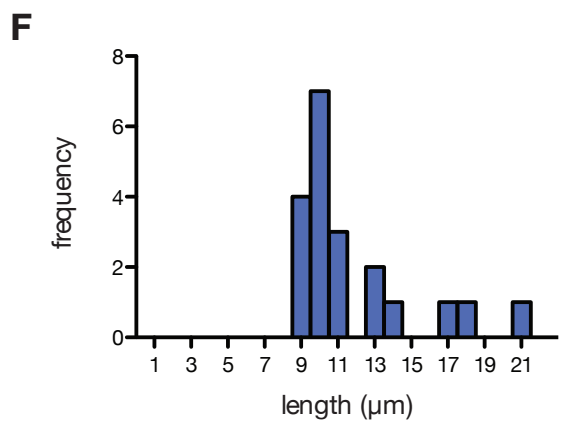
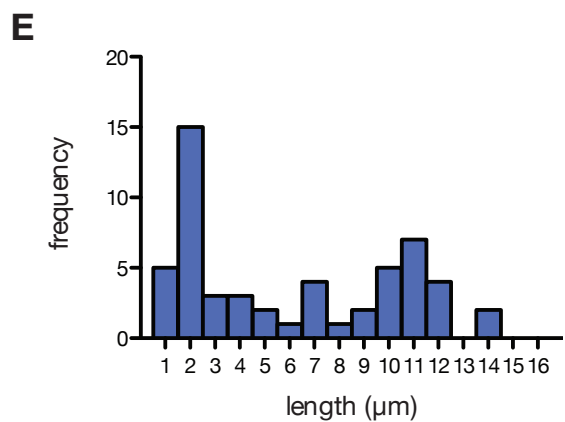
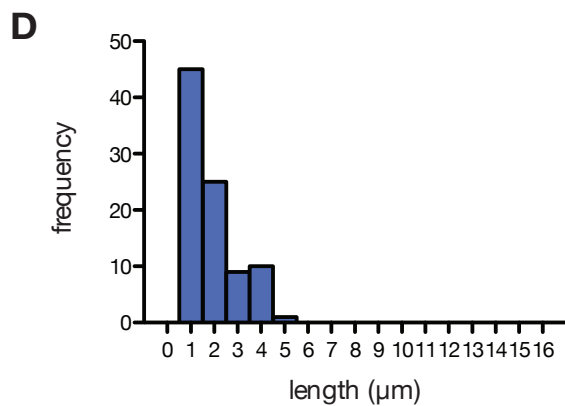
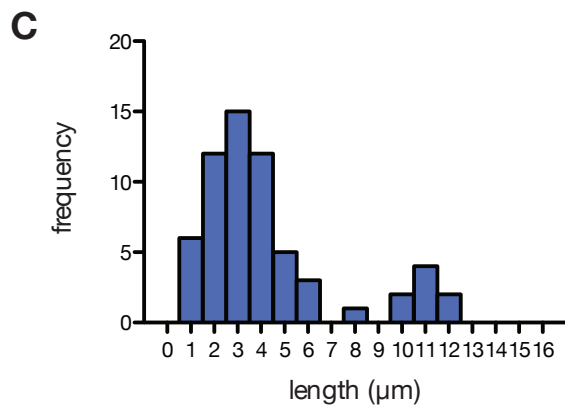
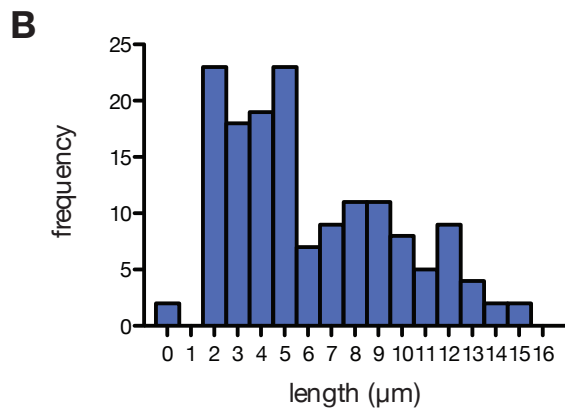
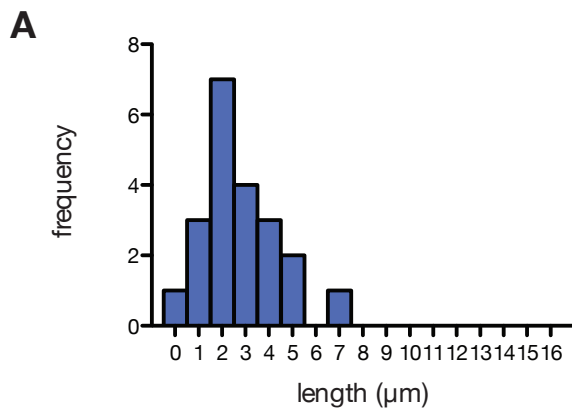


**Figure 3. Flagellar length distributions of canonical *shf* mutants**

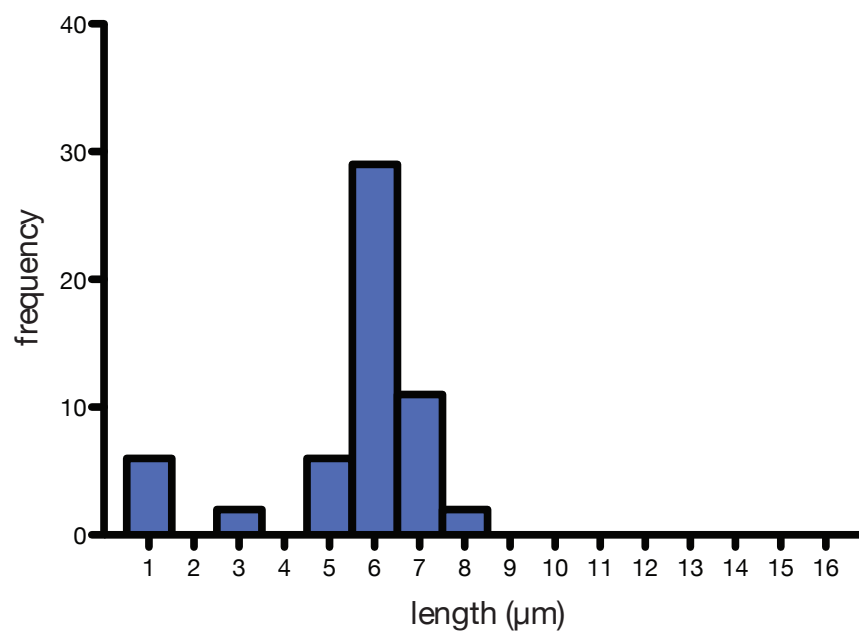
Cells were fixed in glutaraldehyde prior to visualization and measurement of flagella.

Flagellar length is expressed as mean  $\pm$  standard error of the mean.

(A) *shf1-253* flagellar length=  $5.15 \pm .29 \mu\text{m}$ , skew= -1.38, kurtosis= .42 (N= 60 flagella)

(B) *shf3-1851* flagellar length=  $10.39 \pm .15 \mu\text{m}$ , skew= -.35, kurtosis= -.26 (N= 60 flagella)

**A**



**B**

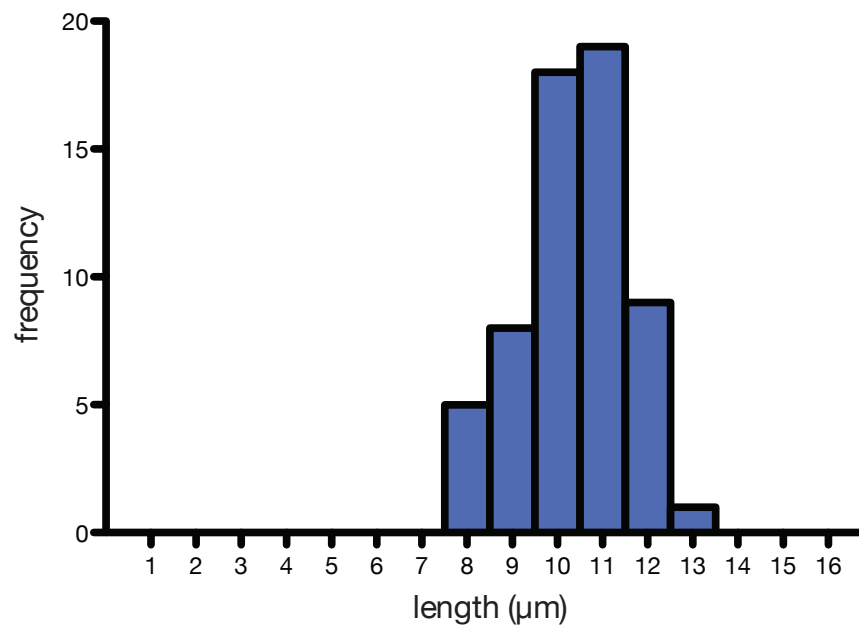


**Figure 4. Images of wild type and selected insertional *shf* mutants**

Cells were fixed in glutaraldehyde and imaged with DIC optics at 60x magnification.

(A) Wild type strain cc-125

(B) Insertional *shf* mutants

**A**



**B**



**Figure 5. Flagellar length distributions of Class I insertional *shf* mutants**

Class I is defined by positive skew and positive kurtosis. Cells were fixed in glutaraldehyde prior to visualization and measurement of flagella.

(A) Strain 802 (N= 114 flagella)

(B) Strain 267 (N= 110 flagella)

(C) Strain 6648 (N= 49 flagella)

(D) Strain 6773 (N= 50 flagella)

(E) Strain 5834 (N= 110 flagella)

(F) Strain 5840 (N= 39 flagella)

(G) Strain 5836 (N= 60 flagella)

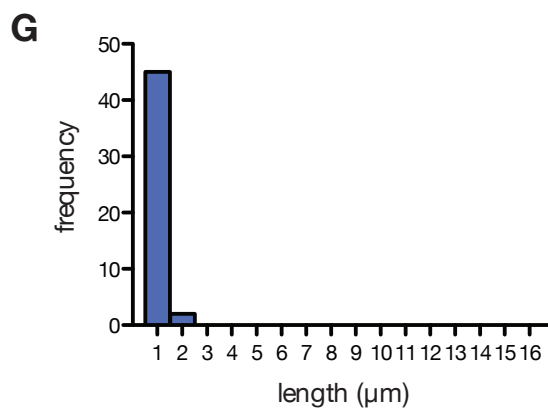
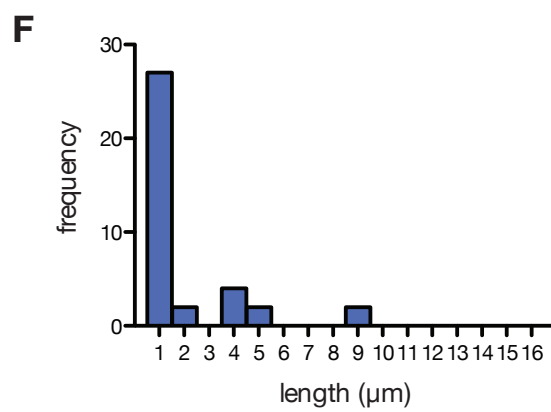
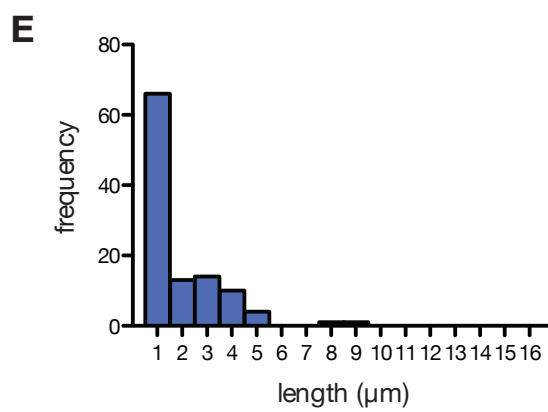
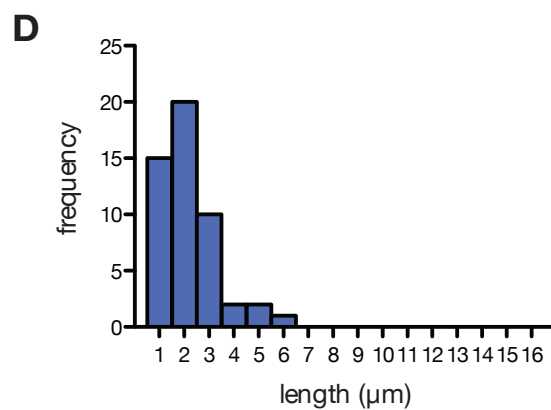
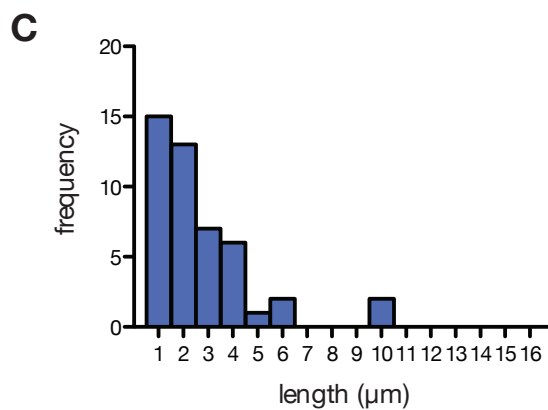
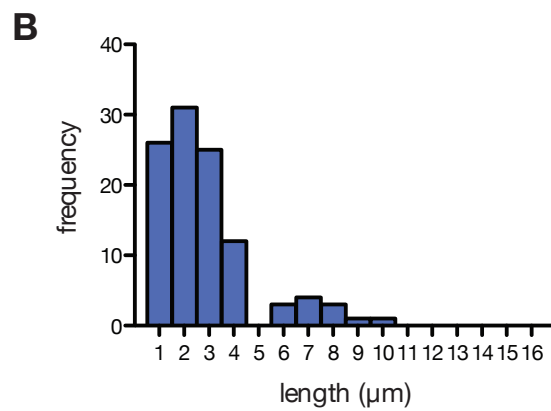
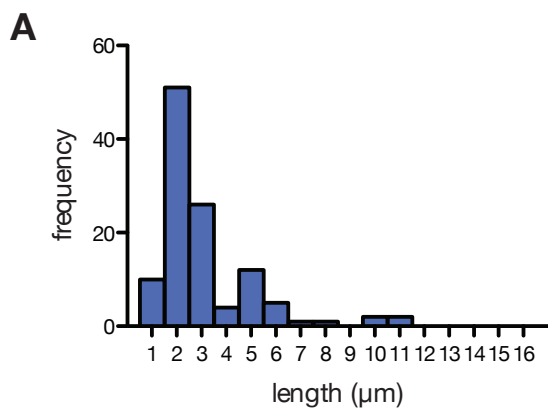




**Figure 6. Flagellar length distributions of Class II insertional *shf* mutants**

Class II is defined by negative skew and positive kurtosis. Cells were fixed in glutaraldehyde prior to visualization and measurement of flagella.

(A) Strain 9111 (N= 109 flagella)

(B) Strain 7107 (N= 130 flagella)

(C) Strain 9484 (N= 108 flagella)

(D) Strain 6894 (N= 110 flagella)

(E) Strain 8488 (N= 110 flagella)

(F) Strain 8333 (N= 114 flagella)

(G) Strain 6444 (N= 112 flagella)

(H) Strain 8796 (N= 83 flagella)

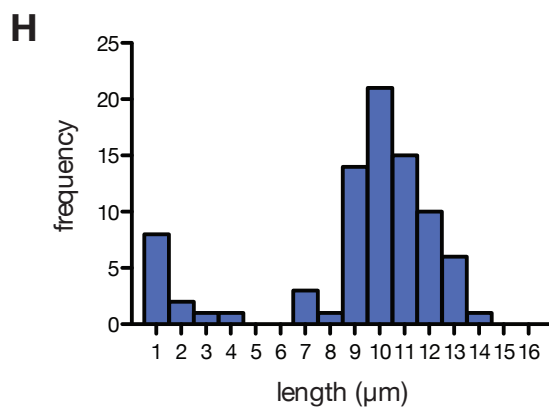
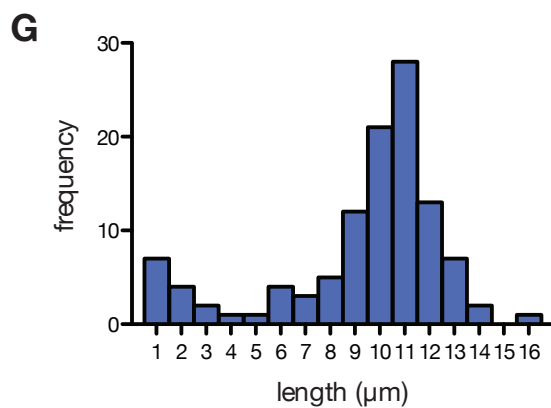
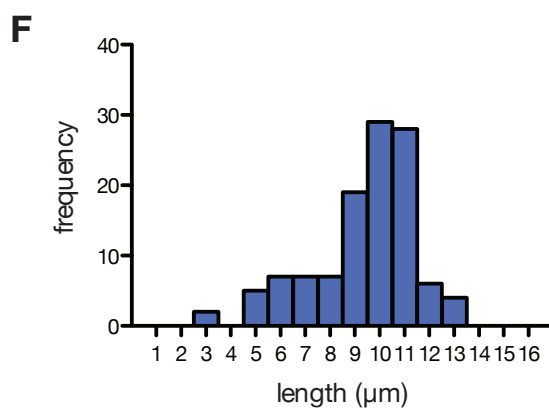
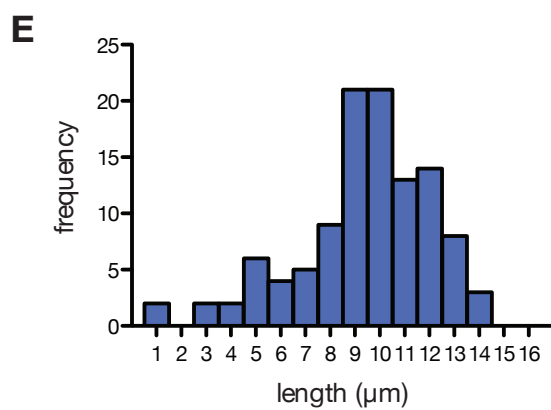
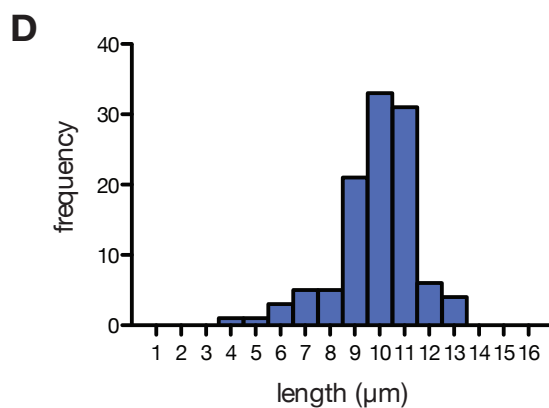
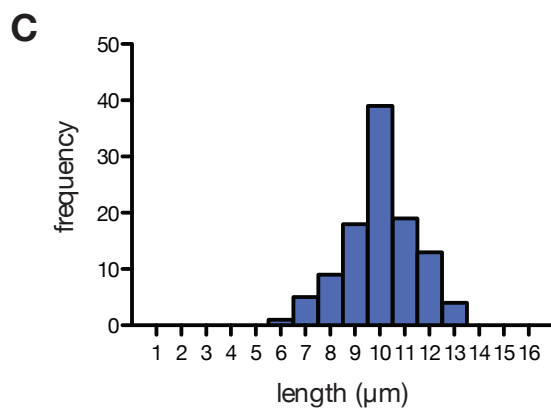
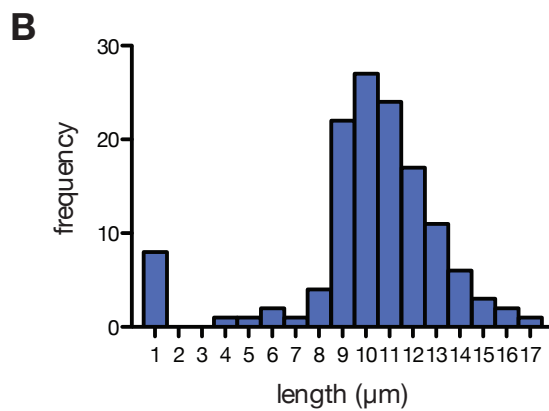
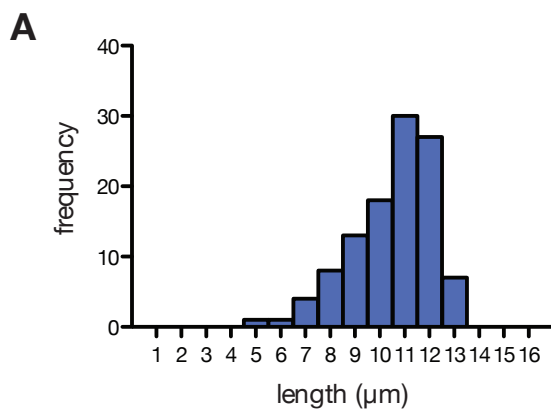


**Figure 7. Flagellar length distributions of Class III insertional *shf* mutants**

Class III is defined by negative kurtosis. Cells were fixed in glutaraldehyde prior to visualization and measurement of flagella.

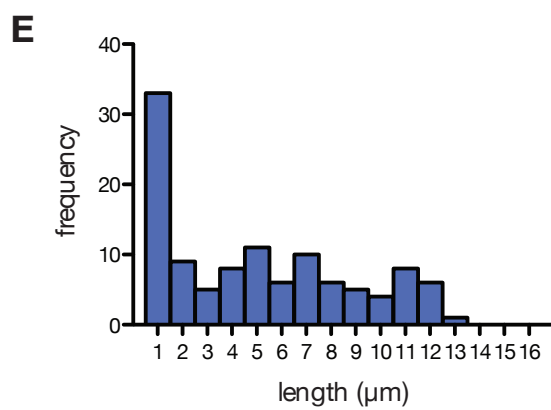
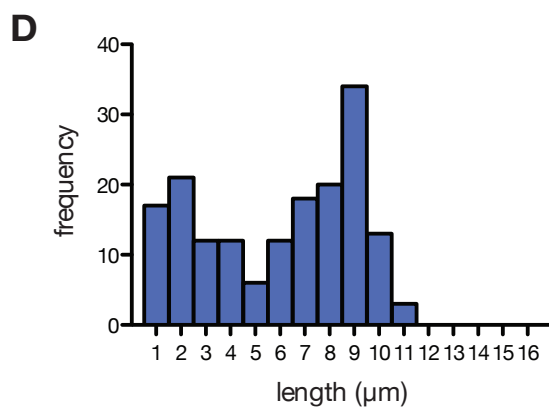
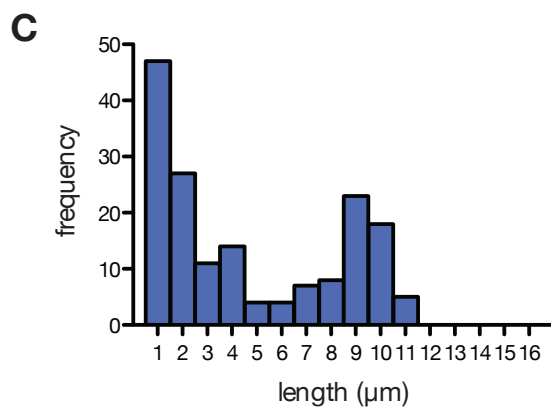
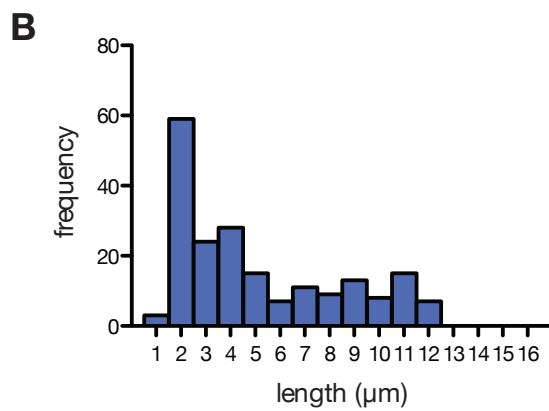
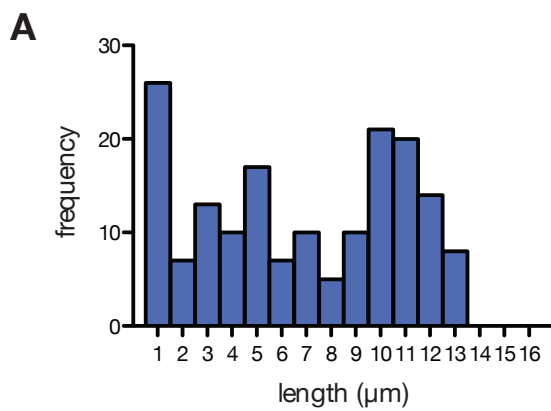
(A) Strain 784 (N= 168 flagella)

(B) Strain 4580 (N= 170 flagella)

(C) Strain 1464 (N= 199 flagella)

(D) Strain 5899 (N= 112 flagella)

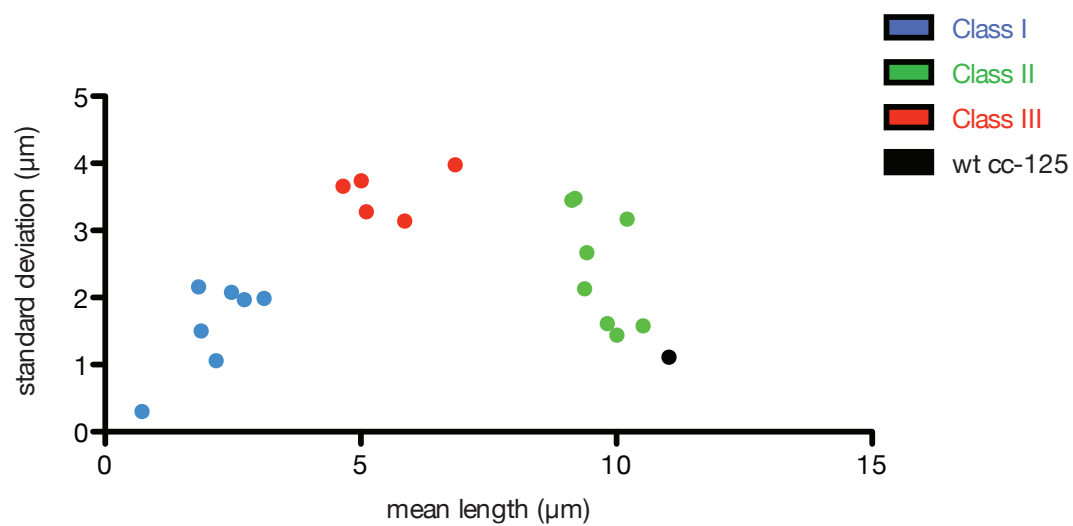
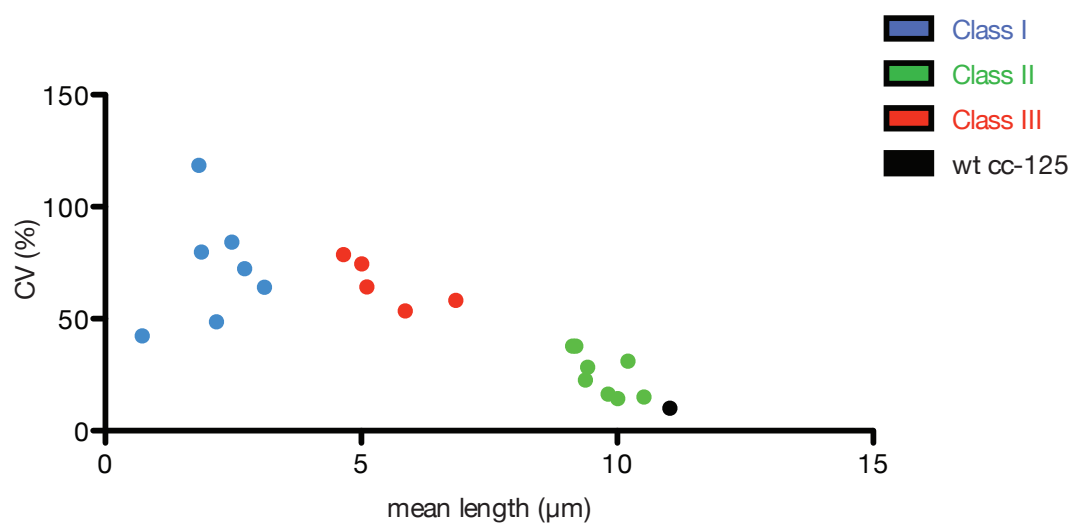
(E) Strain 3584 (N= 170 flagella)



**Figure 8. Relationships between flagellar length and variability**

Length measurement data from Figures 1, 5, 6, and 7 was used to compare mean flagellar length with the standard deviation and coefficient of variation. Each point represents a single strain, of which  $\geq 39$  flagella were measured.

- (A) Class III mutant distributions (red) have higher standard deviations than wild type (black), Class I mutants (blue) and Class II mutants (green).
- (B) There is a negative correlation between mean flagellar length and coefficient of variation ( $r^2 = .6478$ ,  $p < .0001$ )

**A****B**

**Figure 9. Regenerating flagella assume a typical length distribution**

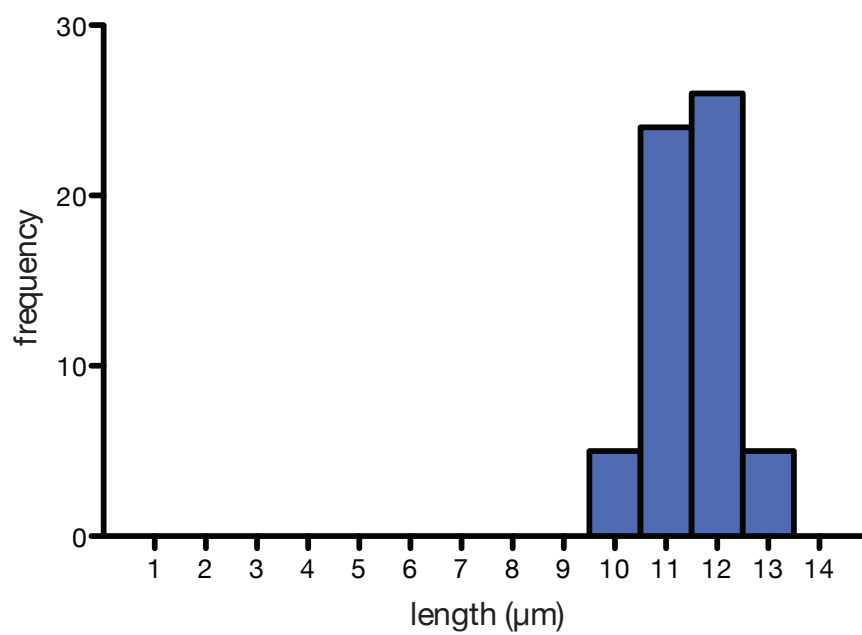
The length distribution of regenerated flagella is similar to the pre-shock distribution.

Wild type cells were deflagellated by pH shock and allowed to regenerate flagella for two hours before visualization and measurement.

(A) Flagellar length distribution prior to pH shock (N= 60 flagella)

(B) Flagellar length distribution after pH shock and recovery (N= 60 flagella)

**A**



**B**

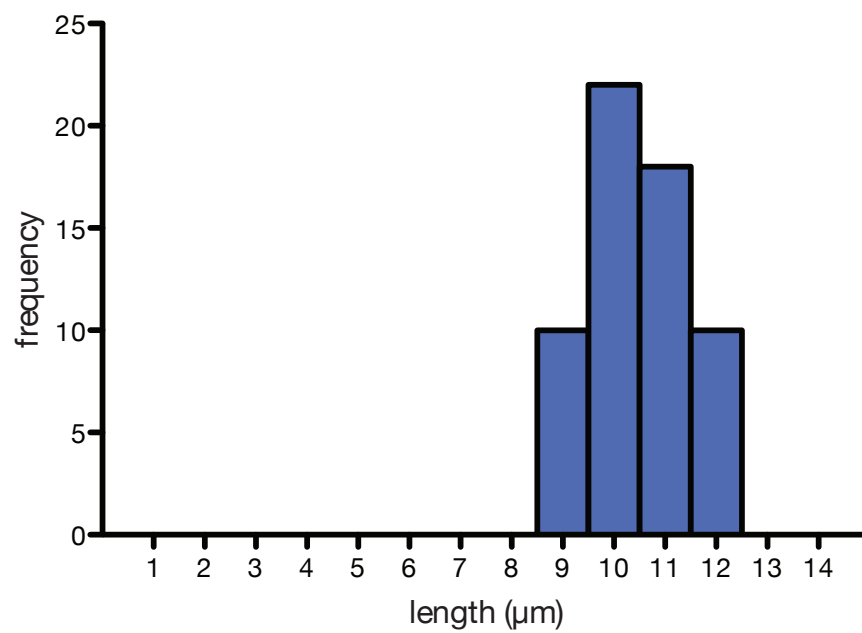




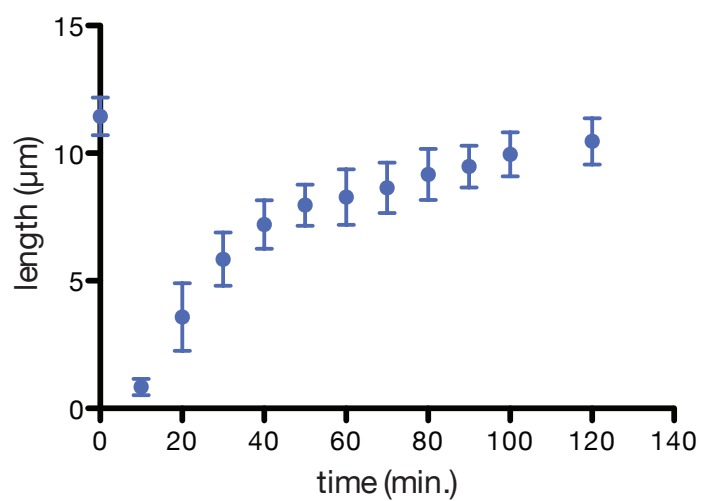
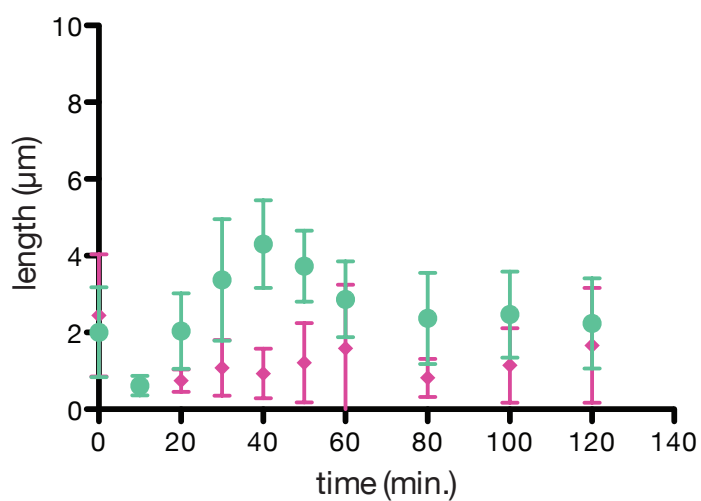
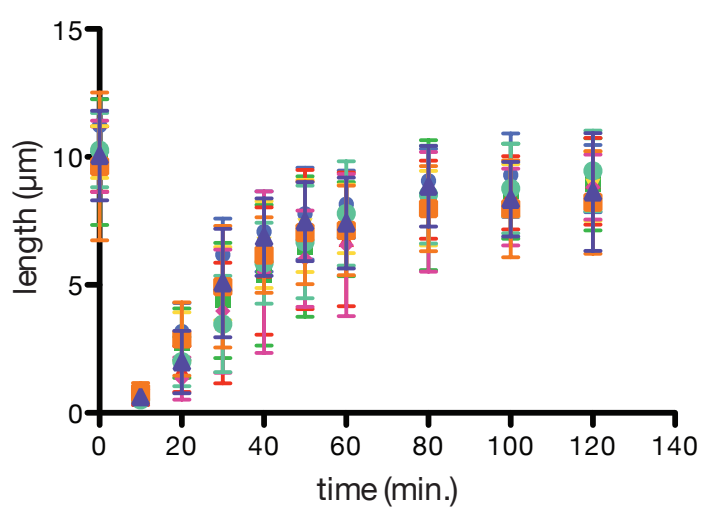
**Figure 10. Flagellar regeneration kinetics of wild type strain, Class I, and Class II *shf* mutants**

Cells were deflagellated by pH shock and permitted to regenerate flagella. Flagellar length is shown as a function of time, with deflagellation occurring at  $t=0$ . Pre-shock length is indicated at the zero time point. In all cases pH shock caused complete removal of flagella (length= 0 $\mu$ m). Data are represented as mean length  $\pm$  standard deviation, with  $N \geq 60$  flagella at each time point.

(A) Wild type strain cc-125

(B) Class I mutants

(C) Class II mutants

**A****B****C**

**Figure 11. Regeneration kinetics of Class III *shf* mutants suggest a defect with the flagellar precursor pool**

Cells were deflagellated by pH shock and permitted to regenerate flagella. Flagellar length is shown as a function of time, with deflagellation occurring at  $t=0$ . Pre-shock length is indicated at the zero time point. In all cases pH shock caused complete removal of flagella (length= 0 $\mu$ m). Data are represented as mean length  $\pm$  standard deviation.

(A) Wild type strain cc-125 typically regenerates with decelerating kinetics (blue circles).

Addition of 10 $\mu$ g/ml cycloheximide to both shock and recovery media prevents new protein synthesis such that the length of regenerated flagella indicates the functional amount of any pre-existing flagellar precursors (red squares). The lack of flagellar growth after 40 minutes indicates that the steady state pool of flagellar precursors has been exhausted. ( $N \geq 37$  flagella at each time point)

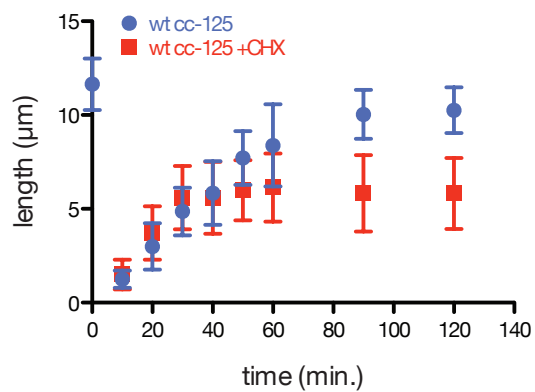
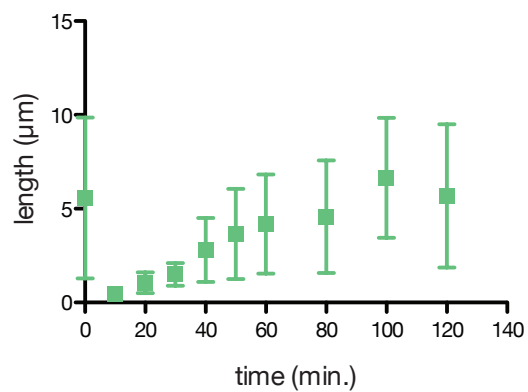
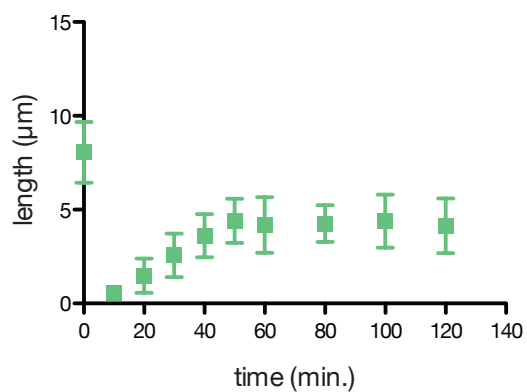
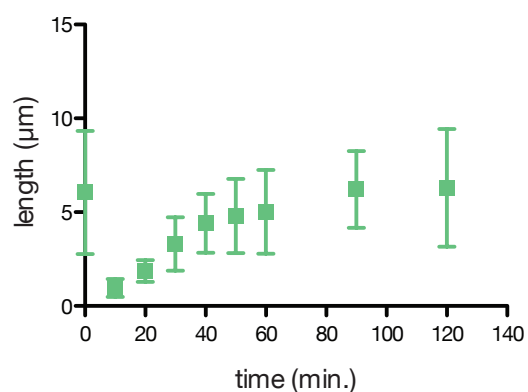
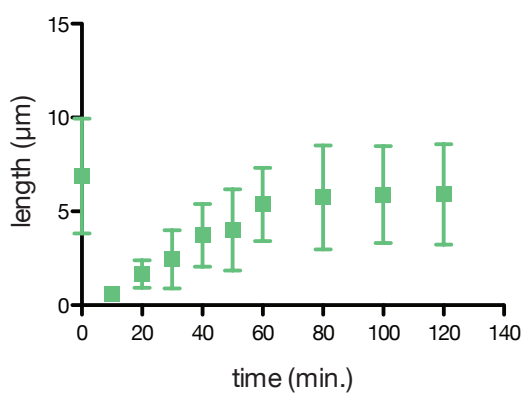
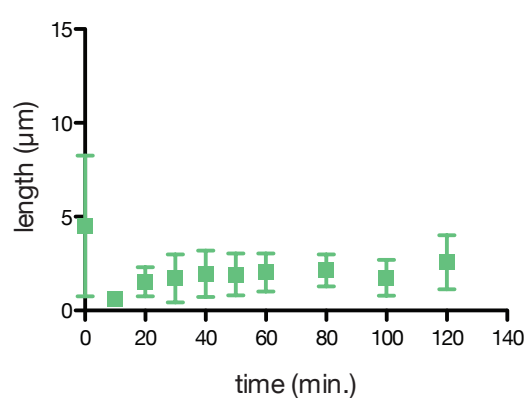
(B) Strain 784 exhibits slow initial growth. ( $N \geq 60$  flagella at each time point)

(C) Strain 4580 exhibits slow initial growth, and cessation of growth after approximately 50 minutes. ( $N \geq 60$  flagella at each time point)

(D) Strain 1464 exhibits slow initial growth, with limited growth after approximately 60 minutes. ( $N \geq 60$  flagella at each time point)

(E) Strain 5899 exhibits slow initial growth, with limited growth after approximately 60 minutes. ( $N \geq 60$  flagella at each time point)

(F) Strain 3584 exhibits little regeneration. ( $N \geq 60$  flagella at each time point)

**A****B****C****D****E****F**

**Figure 12. Estimation of the functional pool size in Class III mutants**

Functional pool size is inferred from the length of flagella regenerated in the absence of protein synthesis. Deflagellation by pH shock and regeneration took place in the presence of 10 $\mu$ g/ml cycloheximide. Flagella were measured two hours after deflagellation. Data are represented as mean length  $\pm$  standard error of the mean, with  $N \geq 40$  flagella. All mutants had significantly smaller steady state pool size than the wild type strain ( $p < .05$ ) as determined by 1-way ANOVA followed by Bonferroni's multiple comparison test.

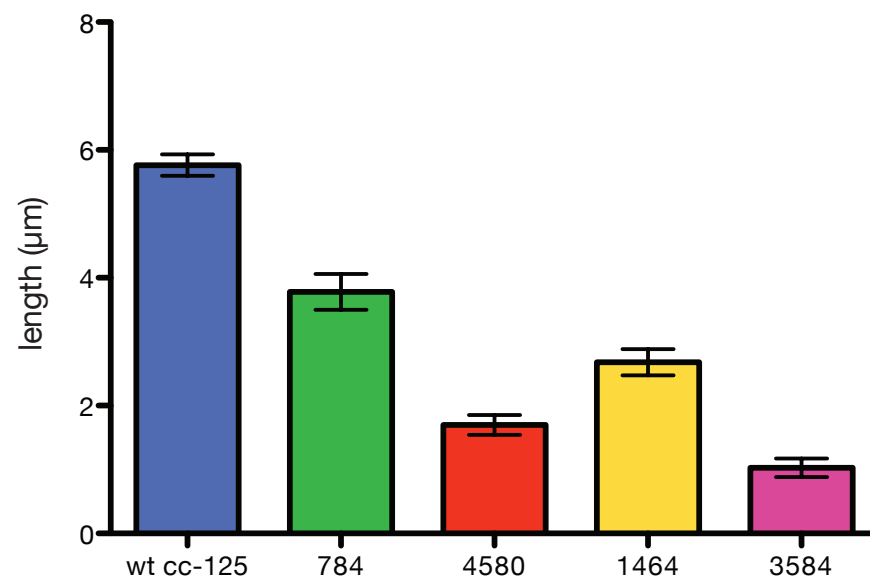


**Figure 13. Dynamics of the functional precursor pool in Class III mutants**

Cells were deflagellated by pH shock and permitted to regenerate flagella. At designated intervals during the regeneration period, cells were subjected to a second deflagellation in the presence of 10 $\mu$ g/ml cycloheximide and permitted to regenerate for two hours in cycloheximide before fixation and measurement of flagella. Final flagellar length is shown as a function of the time of the second deflagellation. Data are represented as mean length  $\pm$  standard error of the mean, with  $N \geq 40$  flagella for each time point. Although there is insufficient data to make a robust statistical comparison of the rate of pool recovery, the data suggest that pool recovery is impaired in the mutant strains.

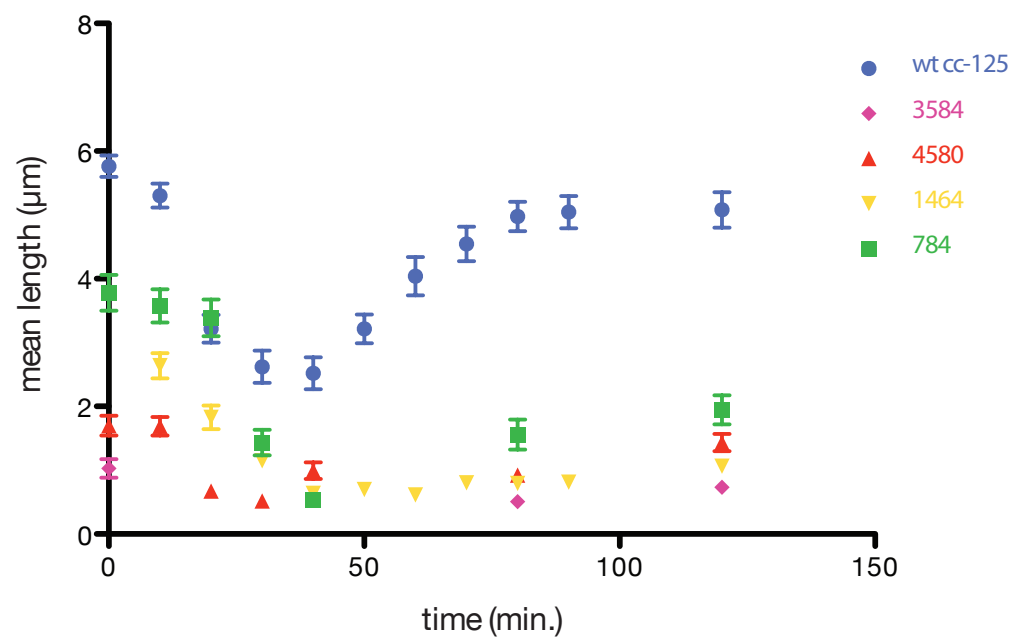




#### Figure 14. Gene expression during flagellar regeneration

Expression of flagellar genes is known to be induced during regeneration. Cells were deflagellated by pH shock and permitted to regenerate flagella. At the designated times, cells were collected and RNA was isolated and reverse transcribed. Gene expression was measured by qPCR. Genes coding for radial spoke protein 3 (*RSP3*), radial spoke protein 6 (*RSP6*), and  $\alpha$ -tubulin (*TUA1*) were normalized to RuBisCo (*RBCS2B*) as an internal control.

- (A) Control experiment shows that *RBCS2B* expression is unchanged during pH shock and flagellar regeneration. Data were collected in four separate experiments and error bars represent the standard deviation within all experiments. There were no significant differences in *RBCS2B* expression within a single experiment or from one experiment to another, as determined by 2-way ANOVA ( $p=.2934$  and  $p=.4533$  respectively).
- (B) Expression of *RSP3* is strongly induced during flagellar regeneration, with maximal expression at 30 minutes post-deflagellation and decreasing expression thereafter. Four experiments are shown and error bars represent the standard deviation within each single experiment.
- (C) Expression of *RSP6* is strongly induced during flagellar regeneration with maximal expression at 30 minutes post-deflagellation and decreasing expression thereafter. Three experiments are shown and error bars represent the standard deviation within each single experiment.

(D) Expression of *TUA1* is induced during flagellar regeneration with variable kinetics.

Three experiments are shown and error bars represent the standard deviation within each single experiment.

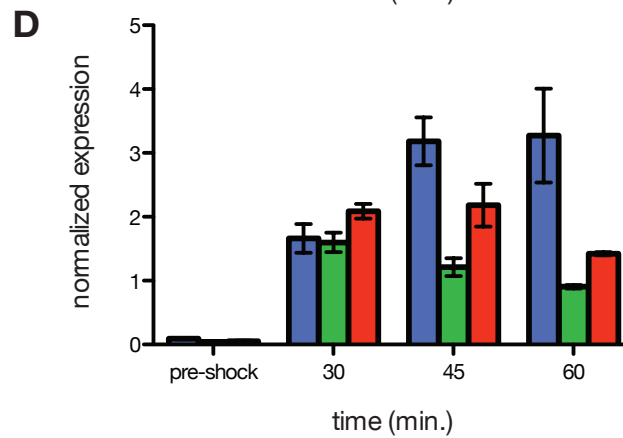
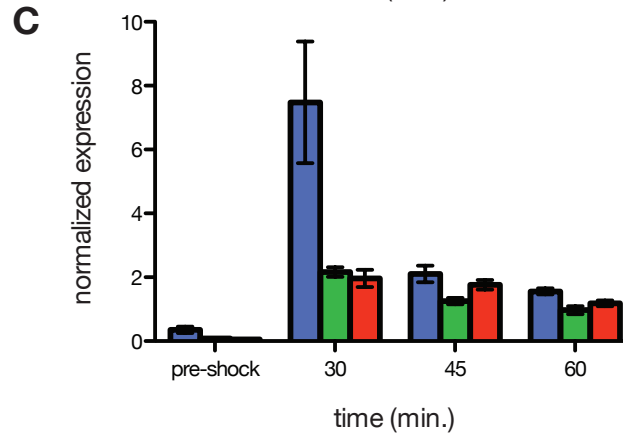
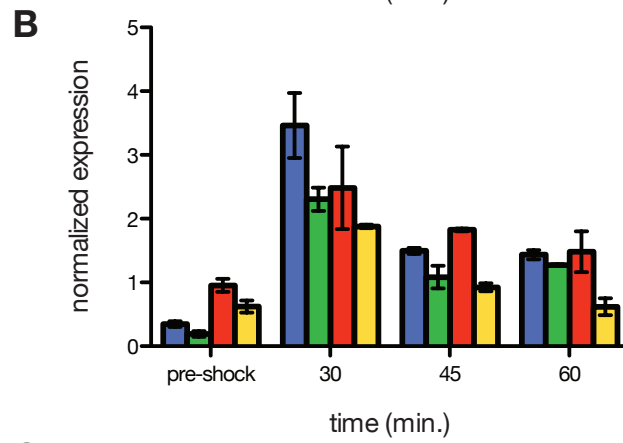
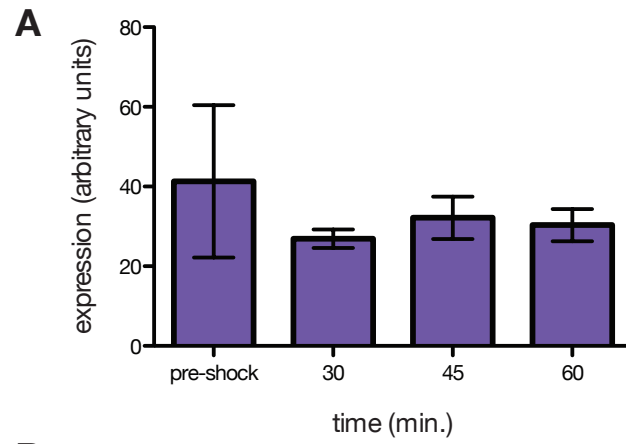


**Figure 15. *RSP3* induction during flagellar regeneration in insertional *shf* mutants**

Cells were deflagellated by pH shock and permitted to regenerate flagella. Cells were harvested 30 minutes after deflagellation and RNA was isolated and reverse transcribed. Gene expression was measured by qPCR and normalized to RuBisCo as an internal control. Error bars represent the standard deviation within a single experiment. Asterisks designate degree of significance from the wild type strain as determined by 1-way ANOVA followed by Bonferroni's multiple comparison test. \* indicates  $p < .01$ , \*\* indicates  $p < .001$ .

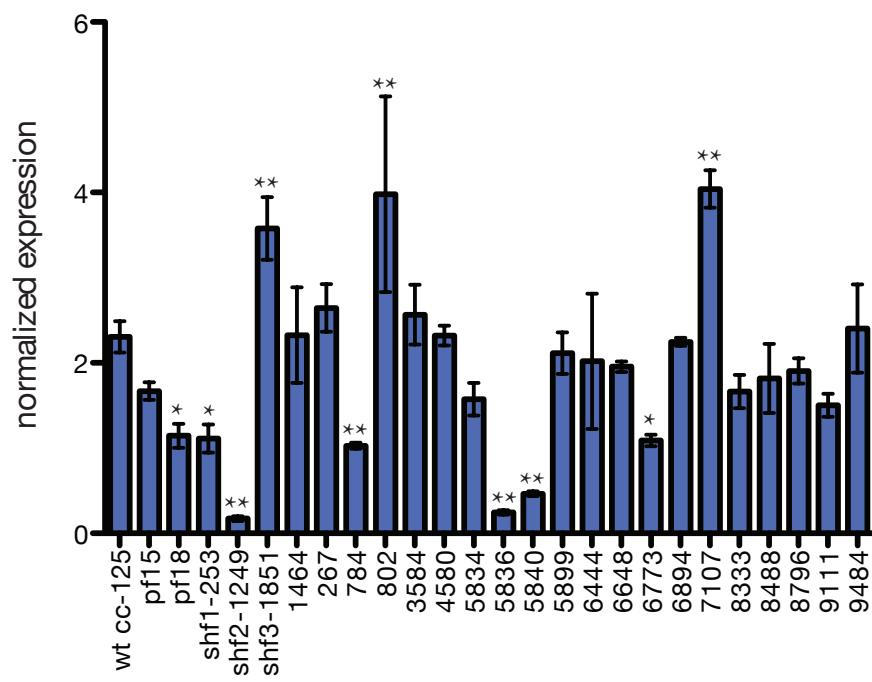


**Figure 16. *RSP3* expression during flagellar regeneration in Class III mutants**

Cells were deflagellated by pH shock and permitted to regenerate flagella. Cells were harvested at the indicated times and RNA was isolated and reverse transcribed. Gene expression was measured by qPCR and normalized to RuBisCo as an internal control. Error bars represent the standard deviation within a single experiment. Asterisks designate significant differences from wild type expression level at the respective time point as determined by 2-way ANOVA followed by Bonferroni's multiple comparison test ( $p < .0001$ ).

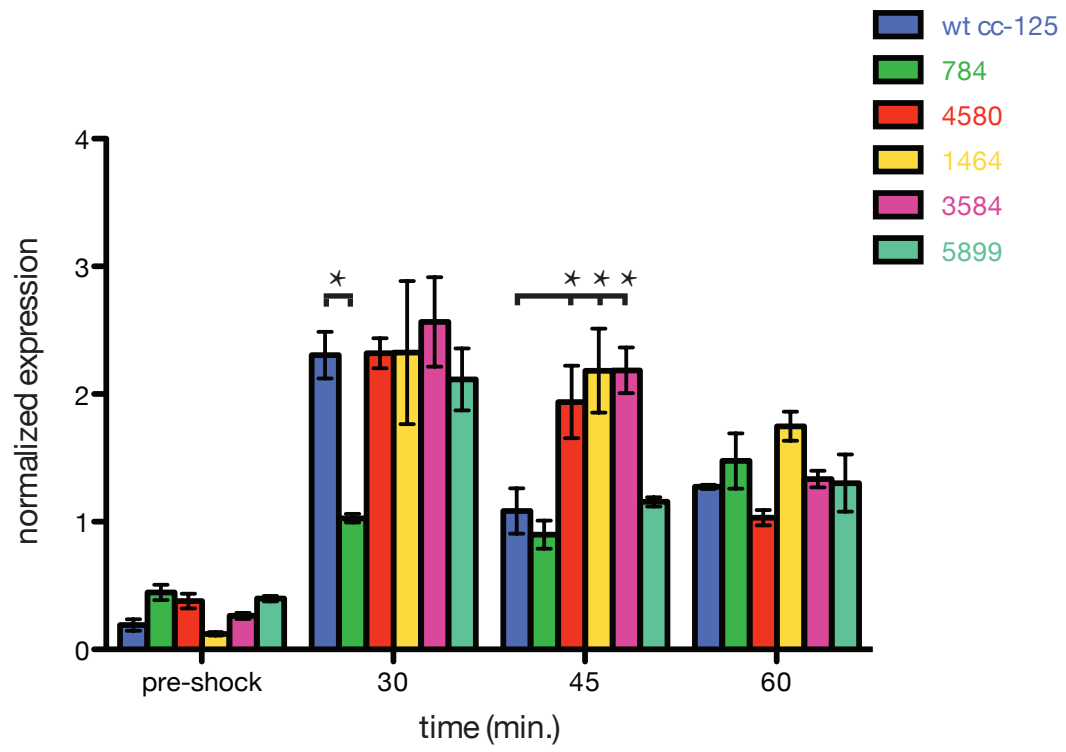


**Table 1. Summary of flagellar length data**

<i>strain</i>	<i>class</i>	<b>Flagellar length characteristics</b>				<b>distribution characteristics</b>	
		mean	standard deviation	maximum	minimum	skew	kurtosis
wild type							
cc-125	-	11.03	1.11	15.06	8.79	0.06	0.43
9111	II	10.52	1.58	12.83	5.29	-0.88*	0.49
7107	II	10.21	3.17	16.63	0.57	-1.23*	2.68**
9484	II	10.01	1.44	13.44	6.12	-0.12	0.19
6894	II	9.82	1.61	13.21	4.01	-0.94*	1.72**
8488	II	9.42	2.67	14.19	1.15	-0.81*	0.71
8333	II	9.38	2.13	13.30	2.59	-0.94*	0.74
6444	II	9.19	3.48	15.57	0.47	-1.26*	0.80
8796	II	9.13	3.45	13.73	0.63	-1.48*	1.22**
784	III	6.85	3.98	13.45	0.59	-0.09	-1.42**
4580	III	5.86	3.14	10.81	0.40	-0.28	-1.36**
1464	III	5.11	3.28	12.34	1.31	0.74*	-0.81**
5899	III	5.01	3.74	13.04	0.64	0.49*	-1.05**
3584	III	4.65	3.66	11.36	0.37	0.43*	-1.46**
802	I	3.11	1.99	11.46	0.96	2.15*	5.28**
267	I	2.72	1.97	9.94	0.43	1.70*	2.74**
6648	I	2.47	2.08	9.98	0.45	2.01*	4.97**
6773	I	2.17	1.06	5.66	0.86	1.25*	1.82**
5834	I	1.88	1.50	8.76	0.45	2.01*	5.16**
5840	I	1.83	2.16	9.37	0.41	2.29*	4.98**
5836	I	0.72	0.30	1.91	0.37	1.74*	3.67**

\* indicates significant deviation from normality, defined as a skewness statistic with absolute value greater than twice the standard error of skew

\*\* indicates significant deviation from normality, defined as a kurtosis statistic with absolute value greater than twice the standard error of kurtosis



**Table 2. Regeneration characteristics**

strain	class	initial growth rate ( $\mu\text{m}/\text{min}$ )	% regeneration at $t=120$
wild type			
cc-125	-	0.17	91.3%
9484	II	0.16	91.3%
8488	II	0.18	88.1%
9111	II	0.22	81.5%
6894	II	0.19	86.9%
8333	II	0.18	92.1%
7107	II	0.16	91.1%
6444	II	0.18	85.4%
784	III	0.06	63.0%
4580	III	0.09	50.2%
3584	III	0.06	54.1%
5899	III	0.09	85.8%
1464	III	0.09	149.4%

## Chapter 3: A role for katanin in flagellar length control

In the previous chapter, I described the identification of mutants that have defects in flagellar precursor protein pool synthesis or mobilization. These are, to our knowledge, the first such mutants ever identified. It is thus of great interest to determine that genes and pathways are revealed by the mutations in these strains. This chapter describes my efforts to identify the genes affected in our *shf* mutants, subsequent work to further characterize the phenotype of the Class III mutant 1464, and attempts to define a mechanistic link between the microtubule severing protein katanin and short flagella.

## INTRODUCTION

The feasibility of genetic and molecular biology techniques in the unicellular biflagellate green alga *Chlamydomonas reinhardtii* renders it an ideal organism for the study of flagellar biology. Wild type *Chlamydomonas* flagella are 10-12µm in length, and protrude through the cell wall at the anterior end of the cell. The fine structure of the axoneme has been well characterized and more than 360 components have been discovered utilizing proteomic and two-dimensional electrophoresis approaches (Luck et al., 1977; Pazour et al., 2005). Additionally, the *Chlamydomonas* genome has been sequenced and annotated (Merchant et al., 2007).

Genetic screens in *Chlamydomonas* have historically used chemical, ultraviolet, and insertional mutagenesis. One of the main advantages of insertional mutagenesis is that by its nature, the molecular lesion has a defined sequence signature. This enables a simple PCR-based strategy for identifying the insertion site in the genome. The main challenge is to design an appropriate assay to reveal mutants of interest for the process under consideration.

In *Chlamydomonas*, the two flagella are not essential for viability; cells with nonmotile flagella, flagella of abnormal length, and even cells completely lacking flagella are fully viable. Mutagenesis followed by phenotypic screens for flagellar motility has proven a fruitful way of identifying centriole and flagella mutants. There are several rapid ways of identifying mutants with altered motility; one relies upon phototaxis, in which

the cell swims toward a unidirectional light source. *Chlamydomonas* cells sense light using the eyespot, an organelle located peripherally, near the equator of the cell. The eyespot is associated with the distal end of one of the flagellar roots, giving rise to an asymmetry that enables a shift from tumbling motility to directed motility in response to phototactic signals from the eyespot. Thus, an inability to phototax can signal flagellar defects.

By coupling insertional mutagenesis with a phototaxis assay, a collection of centriole and flagella mutants was obtained as described previously (Feldman et al., 2007). A subset of mutants was determined visually to have short flagella and we attempted to clone the affected genes in these strains in order to identify genes involved in flagellar length control. These mutants were described in detail in the preceding chapter.

We were able to identify sequence flanking the insertion in four mutants. Of the identified genomic regions, only one insertion occurred in a well-characterized gene, *PF15*. The *pf15* strain was one of the first flagellar motility mutants to be isolated in *Chlamydomonas* and was shown to have paralyzed flagella that lack the central pair of microtubules (Warr et al., 1966). The *PF15* gene was later cloned, and found to encode the p80 subunit of the microtubule severing heterodimer katanin (Dymek et al., 2004). Although it is known that *pf15*, along with the central pair-deficient strains *pf18*, *pf19*, and *pf20*, lacks 18 axonemal polypeptides (Adams et al., 1981), and work in *Tetrahymena* has implicated katanin in ciliary assembly and posttranslational modification of ciliary microtubules (Sharma et al., 2007), its mechanism of action with respect to flagellar phenotypes has remained unclear.

Our novel mutant strain was originally classified as a short flagella mutant (*shf*), in contrast to previously published reports stating that *pf15* cells possess flagella of normal length. We have attempted to elucidate how katanin p80 affects flagellar length by investigating flagellar regeneration, transcriptional upregulation during flagellar regeneration, dynamics of the flagellar precursor pool, resistance of cells to microtubule toxins, and tubulin polymer content.

## RESULTS

### *Mapping and identification of katanin p80 mutation in shf strain 1464*

To determine the regions flanking the inserted sequence in our collection of insertional mutants, we utilized restriction enzyme site-directed amplification PCR (RESDA-PCR) (Gonzalez-Ballester et al., 2005). Our RESDA-PCR results identified flanking sequence in four mutants: 1464, 3584, 4580, and 9111 (Table 1). Of the identified genomic regions, only one insertion occurred in a well-characterized gene (Figure 1). Because of this fact and a known role for the identified gene, *PF15* katanin p80, in flagellar biology, subsequent experiments to elucidate molecular mechanisms of length control focused upon mutant 1464.

In *Chlamydomonas*, insertion of foreign sequence is often accompanied by a deletion of surrounding sequence (Harris, 1989). In practice, it is important to determine whether it is indeed the inserted sequence that causes the observed phenotype. This was achieved for mutant 1464 by mating the mutant strain to a wild type strain, followed by tetrad dissection using established techniques. Consistent with a role for katanin p80 in meiosis (Srayko et al., 2000), very few complete tetrads were obtained. The genotype and phenotype of 135 random progeny were assessed using a quadruple-redundant PCR strategy to identify the presence of an insertion and a visual screen for flagellar length and motility. No recombinants were identified, giving a LOD score of ~40 and certainty that the insertion causes the phenotype in mutant 1464.

### ***Shf strain 1464 shares phenotype with katanin p80 subunit point mutant***

Because prior studies had stated that the *pf15* strain lacked the central pair of microtubules, we wished to investigate whether mutant 1464 had a central pair defect as well. Our collaborator Sebastian Schuck prepared cells for cryo-electron microscopy and found that 0/20 cells contained the central pair (Figure 2), a virtually identical phenotype to that seen in *pf15* mutants. Given that the insertional katanin 80 mutant phenocopied the central pair defect of *pf15*, we wished to investigate whether the original isolate of *pf15* also gave rise to the *shf* phenotype characterized for strain 1464 in the preceding chapter.

The *pf15* strain contains a point mutation in the second exon of the *PF15* gene, giving to a single amino acid substitution, V43D (Dymek et al., 2004). In contrast to published results, and as discussed in the preceding chapter, we found that the *pf15* strain does exhibit heterogeneous flagellar lengths with a platykurtic distribution. Subsequent experiments showed that *pf15* also phenocopies the 1464 mutant with respect to regeneration kinetics and the defect in regenerating the functional pool of flagellar precursors, and both mutant strains induce *RSP3* expression similarly to the wild type strain (Figure 3). Although we did not rescue our insertional mutant with the wild type *PF15* gene, the identical phenotypes of our insertional mutant, with its large deletion, and the *pf15* point mutant indicate that *PF15* mutation is indeed the cause of the *shf* phenotype with an underlying defect in precursor pool regeneration.



### ***Investigation of effect of katanin p80 mutation on microtubule stability***

In order to determine the effect of katanin p80 mutation on cell growth, we cultured cells on solid media containing either the depolymerizing herbicide oryzalin ((James et al., 1993) or the hyperstabilizing agent taxol. Neither the insertional mutant 1464 nor the *pfl5* strain showed enhanced resistance or susceptibility to the anti-microtubule agents as compared to a wild type strain (Figure 4, taxol data not shown), suggesting that the effect of the mutations on microtubule dynamics, if any, may be fairly subtle. It should be noted, however, that taxol is less effective in most algae, including *Chlamydomonas*, so a negative result for taxol sensitivity is not informative.

We hypothesized that katanin p80 could play a role in regulating the partitioning of tubulin between the cytoskeleton and axoneme, and that short flagella in mutant 1464 were due to a lack of tubulin available for incorporation into flagella. To test this hypothesis, we lysed and fractionated cells to see if there was altered tubulin polymer content in mutant 1464. Results from a single experiment are shown in Figure 5, but the slight increase in tubulin polymer content in mutant 1464 and *pfl5* was not statistically significant and the result was not reproducible. It is likely that the assay was not reproducible due to the complicated sample preparation. *Chlamydomonas* cells possess a rigid cell wall, necessitating bead beating for complete lysis. It is possible that physical forces or fluctuations in temperature during bead beating (typically done in intervals, while placing the samples on ice between beating steps) may have affected the microtubule cytoskeleton. It is also possible that an incorrect concentration of taxol was used in the buffer. An alternative method that would be recommended for future studies

is to image cytoplasmic microtubules using 3D microscopy and measure their length to see if there are any alterations during steady state or flagellar regeneration. Our initial attempts to obtain such images were not successful due to the limited resolution of the microscope, which could not resolve individual microtubules. However, recent advances in super-resolution imaging may provide a way to successfully perform this analysis in the future.

## DISCUSSION

Katanin is a microtubule-severing heterodimer; p60 is the catalytic subunit and p80 is the regulatory subunit. *In vitro* studies have shown that p60 alone can sever microtubules, and that p80 enhances the efficacy of severing, along with targeting p60 to the centrosome (Hartman et al., 1998; McNally et al., 2000). Katanin p80, which is disrupted in mutant 1464 and *pf15*, has three characterized domains: an N-terminal WD40 domain that is required for centrosomal localization and has been shown *in vitro* to inhibit severing by p60, a proline-rich central domain, and a conserved C-terminal domain that binds p60 and enhances severing by p60 *in vitro*. Due to the opposing influences of the N-terminal and C-terminal domains, is difficult to make an *a priori* prediction about the effect of either the *pf15* mutation or the 1464 deletion on katanin biochemistry.

Hypotheses about potential phenotypes arising from p80 mutation are further complicated by the fact that katanin has been shown to be both a positive and negative regulator of microtubule mass. Studies of acentrosomal female spindles in *C. elegans* embryos showed that *mei-1(null)* spindles, which have no katanin activity, had greatly reduced polymer mass as compared to wild type spindles (Srayko et al., 2006). However, cultured rat hippocampal neurons overexpressing either p60 or p80 also showed a dramatic reduction in polymer mass, with a more pronounced effect resulting from p60 overexpression (Yu et al., 2005). Because the consequence of microtubule severing is generation of many more plus ends of microtubules, these contrasting effects of katanin

may be explained by differences in the cellular environment that control whether the abundant plus ends polymerize or undergo catastrophe.

Although the molecular effects of katanin mutation are difficult to predict, katanin has been implicated in mitotic spindle length control and modulation of cell length and morphology. Depletion of katanin results in abnormally long metaphase spindles (Goshima and Scholey, 2010). Disruption of a katanin-like protein in *Arabidopsis thaliana*, AtKTN1, gives rise to abnormally short and wide cells that cause a shortening of inflorescence stems, leaves, and floral organs, leading to reduced stature of the overall plant (Burk et al., 2001). Katanin has not specifically been shown to modulate length control of animal cells, but the fundamental role of microtubules in this process suggest this possibility (Picone et al., 2010).

Katanin may exert its effects on modulation of cell morphology by facilitating dramatic remodeling of the microtubule cytoskeleton, a model termed “cut and run” (Baas et al., 2005). The capacity of a microtubule to move is inversely proportional to its length, with only the shortest microtubules displaying rapid concerted motion (Baas and Buster, 2004). The severing action of katanin renders microtubules into small polymers that can move rapidly to a new configuration. Notably, in *Chlamydomonas* growth of flagella immediately follows a major cytoskeletal reorganization: the transition from a mitotic spindle to an interphase array. Regeneration of flagella after abscission can also be considered a major reorganization because of the high demand for free tubulin, which is the major constituent of the axoneme. The classic experiments of Rosenbaum suggest

that tubulin is limiting during regeneration; if only one flagellum is severed, the remaining flagellum is observed to transiently shorten.

Although we were unable to conclusively show how mutation of katanin p80 causes a short flagella phenotype at a biochemical level, recent studies have provided some clues as to a potential mechanism. Sharma and colleagues showed that increasing the pool of soluble tubulin, either by manipulating the actin cytoskeleton or with a carefully titrated dose of nocodazole, correlates with longer cilia in mammalian cells (Sharma et al., 2011). Further insight comes from a recent paper showing that RNAi knockdown of a microtubule depolymerizing kinesin in *Chlamydomonas*, CrKinesin-13, causes a short flagella phenotype, and these cells exhibit atypical regeneration kinetics (Piao et al., 2009). CrKinesin-13 knockdown cells undergo a lag phase of roughly one hour before beginning to regenerate their flagella, after which the flagella grow very slowly, reaching pre-shock length only after four hours, suggesting that mobilization of the flagellar precursor pool is impaired. We have shown that *pfl5* cells have flagella of heterogeneous lengths, with a short mean length, have a defect in regeneration of the flagellar precursor pool, and a slightly higher polymer: soluble tubulin ratio than wild type cells. Taken together, these results suggest a model in which mutation of katanin p80 diminishes severing activity of the katanin heterodimer, leading to stabilization of the microtubule cytoskeleton and a diminished pool of soluble tubulin available for axonemal incorporation, causing a short flagella phenotype.

This type of model is consistent with the idea that within a single cell, there are differentially regulated sets of microtubules with differing functions, such as the stabilized microtubules of the flagellar axoneme and the more dynamic population in the cell body. In the biflagellate golden-brown alga *Ochromonas*, distinct sets of microtubules give rise to different aspects of the cell's characteristic pyriform shape (Brown and Bouck, 1973), and in this system it was clearly shown that as flagella grow, specific sets of cytoplasmic microtubules transiently shorten. Our model of competition between flagellar and cytoplasmic microtubules in *Chlamydomonas* thus has a precedent in *Ochromonas*. Recycling of polymer content to maintain a precursor pool has also been shown to modulate actin dynamics in *Saccharomyces cerevisiae*. The small actin-binding protein cofilin stimulates actin filament severing, and the resulting disassembly products are converted by the cofilin accessory protein Aip1 into monomers and small oligomers that can be incorporated into assembling filaments (Okreglak and Drubin, 2010). An intriguing possibility is that katanin plays a similar role in tubulin polymer recycling in the cytoskeleton and axoneme, such that decreased polymer disassembly results in a shortage of tubulin dimer available for flagellar assembly.

## EXPERIMENTAL PROCEDURES

### *Strains and culture conditions*

*Chlamydomonas reinhardtii* insertional mutants were obtained from Jessica Feldman, and their construction was described previously (Feldman et al., 2007). Strains were maintained on TAP agar plates and experimental cultures grown in M1 liquid media with continuous light and aeration unless otherwise noted.

### *Isolation of genomic DNA*

Two procedures were employed for isolation of genomic DNA: a dual extraction process for harvesting clean genomic DNA for sensitive downstream applications such as RESDA-PCR, and a rapid, crude preparation for genotyping PCR. Clean genomic DNA was obtained utilizing a CTAB/chloroform extraction protocol, followed by a second extraction with phenol chloroform. Cells were grown in TAP media with shaking under continuous light and harvested by centrifugation. Cells were then frozen at -80° C and lyophilized overnight. Lysis was achieved by vortexing with glass beads in CTAB extraction buffer (100mM Tris HCl, pH 7.5, .7M NaCl, 10mM EDTA, 1% CTAB, 1%  $\beta$ -mercaptoethanol), followed by incubation at 65°C for two hours. Subsequent chloroform extraction, isopropanol precipitation, phenol chloroform precipitation, and ethanol precipitation were performed using established techniques. The resulting DNA was treated with 50 $\mu$ g/ml RNase A at 37°C for one hour and .5mg proteinase K at 55°C for one hour. Crude DNA was prepared using a modified smash-and-grab protocol for *Saccharomyces cerevisiae*. Briefly, cells were simultaneously lysed and extracted by

vortexing with glass beads in breaking buffer (2% Triton X-100, 1% SDS, 100mM NaCl, 10mM Tris HCl pH 8.0, 1mM EDTA pH 8.0) and equal volumes of phenol and water.

### ***Identification of flanking sequence***

RESDA-PCR was performed as described in Gonzalez-Ballester et al. using the following primers specific for the mutagenizing plasmid:

HYG 5' R7 TTGCCGGGAAGCTAGAGTAAG

HYG 5' R9 GCCATCCGTAAGATGCTTTTC

HYG 5' R6 ATACGGGAGGGCTTACCATCT

HYG 3' F6 CAGAGGTTTTTCACCGTCATCA

HYG 3' F8 CGAGTGGGTTACATCGAACTG

HYG 3' F5 GCTGCATGTGTCAGAGGTTTT

HYG 3' F7 TTTTGCCTTCCTGTTTTTGCT

Nested PCR products were subjected to gel electrophoresis, followed by excision of discrete bands. PCR products were isolated using a gel purification kit (Qiagen), cloned using a TOPO-TA cloning system (Invitrogen) and sequenced. Identified sequence was compared to the *Chlamydomonas* genome version 3.0.

### ***Genotyping PCR***

Primer pairs were designed such that products specific for the presence or absence of the insertion identified in mutant 1464, located in genomic scaffold 34, would be amplified.



1464 insert+ F1 GACACCAGTCGTCGGTGGAGAGTGT

1464 insert+ R1 TCCGTGTCGCCCTTATTCCTTTT

1464 insert- F1 AGCTTTGTAAAGTGGAGGGGGCAACC

1464 insert- R1 GAGGTGTATGGGGTTGTTGCCGAGT

### ***Motility phenotype assessment***

After two days in liquid culture, aliquots of live cells were subjected to DIC microscopy using a 20x objective and swimming behavior was assessed visually.

### ***LOD score calculation***

The following equation was used to assess the odds of linkage between genotype and phenotype:

$$LOD = \log_{10} \frac{(1 - \Theta)^{NR} \Theta^R}{.5^{(NR+R)}}$$

NR denotes the number of non-recombinant progeny, R denotes the number of

recombinant progeny, and  $\Theta$  is the recombinant fraction  $\frac{R}{NR + R}$

A LOD score of 3 indicates 1000 to 1 odds that the observed linkage did not occur by chance. In practice, a LOD score greater than 3 is considered evidence for linkage.

### ***Cryo-electron microscopy***

Sample preparation and microscopy were performed as described previously (Schuck et al., 2009).

### ***Microtubule drug resistance assay***

TAP agar was prepared and autoclaved as described previously (Harris, 1989). Prior to pouring plates, the desired drug was added to the medium (oryzalin at final concentrations of 2-40 µg/ml; taxol at final concentrations of 2-7 µg/ml). Cells were streaked onto cooled plates and incubated in constant light for one week before growth was assessed visually.

### ***Tubulin polymer assay***

Cells were collected by gentle centrifugation for two minutes at 1500 x g. Flagella were removed by pH shock as described previously, and cells pelleted once more. Cells were resuspended in taxol buffer (100mM tris pH 6.8, 700mM NaCl, 5mM MgCl<sub>2</sub>, 10mM EGTA, 40µg/ml taxol, 1x protease inhibitor cocktail) to stabilize polymerized microtubules and lysed by bead beating. The total protein concentration for each sample was equalized prior to a 10-minute centrifugation at 12,000 x g and 4°C to separate polymerized microtubules and soluble tubulin (Minotti et al., 1991). Supernatant was removed and pelleted cytoskeletons were resuspended in an equal volume of taxol buffer. SDS sample buffer was added and samples were boiled for five minutes. SDS-PAGE was performed using 10% acrylamide gels in a Mini-PROTEAN electrophoresis system (Bio-Rad).

### ***Quantitative western blotting***

Proteins were transferred from acrylamide gels to nitrocellulose membranes using a Trans-Blot SD semi-dry transfer system (Bio-Rad). Blocking, primary antibody, and secondary antibody incubations were performed at room temperature with gentle agitation for one hour. Membranes were blocked with LI-COR blocking buffer (LI-COR Biosciences), incubated with anti- $\alpha$ -tubulin DM1A (Sigma), washed three times for 10 minutes each in TBS, incubated with IRDye 800CW goat anti-mouse IgG (LI-COR Biosciences), and washed three times for 10 minutes each in TBS prior to visualization and analysis using the Odyssey IR imaging system (LI-COR Biosciences).

### ***Statistical analysis***

Statistical tests were performed using GraphPad Prism software.

## REFERENCES

- Adams, G.M., B. Huang, G. Piperno, and D.J. Luck. 1981. Central-pair microtubular complex of *Chlamydomonas* flagella: polypeptide composition as revealed by analysis of mutants. *J Cell Biol.* 91:69-76.
- Baas, P.W., and D.W. Buster. 2004. Slow axonal transport and the genesis of neuronal morphology. *J Neurobiol.* 58:3-17.
- Baas, P.W., A. Karabay, and L. Qiang. 2005. Microtubules cut and run. *Trends Cell Biol.* 15:518-524.
- Brown, D.L., and G.B. Bouck. 1973. Microtubule biogenesis and cell shape in *Ochromonas*. II. The role of nucleating sites in shape development. *J Cell Biol.* 56:360-378.
- Burk, D.H., B. Liu, R. Zhong, W.H. Morrison, and Z.H. Ye. 2001. A katanin-like protein regulates normal cell wall biosynthesis and cell elongation. *Plant Cell.* 13:807-827.
- Dymek, E.E., P.A. Lefebvre, and E.F. Smith. 2004. PF15p is the *Chlamydomonas* homologue of the Katanin p80 subunit and is required for assembly of flagellar central microtubules. *Eukaryot Cell.* 3:870-879.
- Feldman, J.L., S. Geimer, and W.F. Marshall. 2007. The mother centriole plays an instructive role in defining cell geometry. *PLoS Biol.* 5:e149.
- Gonzalez-Ballester, D., A. de Montaigu, A. Galvan, and E. Fernandez. 2005. Restriction enzyme site-directed amplification PCR: a tool to identify regions flanking a marker DNA. *Anal Biochem.* 340:330-335.
- Goshima, G., and J.M. Scholey. 2010. Control of mitotic spindle length. *Annu Rev Cell Dev Biol.* 26:21-57.

- Harris, E.H. 1989. The Chlamydomonas sourcebook : a comprehensive guide to biology and laboratory use. Academic Press, San Diego. xiv, 780 p. pp.
- Hartman, J.J., J. Mahr, K. McNally, K. Okawa, A. Iwamatsu, S. Thomas, S. Cheesman, J. Heuser, R.D. Vale, and F.J. McNally. 1998. Katanin, a microtubule-severing protein, is a novel AAA ATPase that targets to the centrosome using a WD40-containing subunit. *Cell*. 93:277-287.
- James, S.W., C.D. Silflow, P. Stroom, and P.A. Lefebvre. 1993. A mutation in the alpha 1-tubulin gene of Chlamydomonas reinhardtii confers resistance to anti-microtubule herbicides. *J Cell Sci*. 106 ( Pt 1):209-218.
- Luck, D., G. Piperno, Z. Ramanis, and B. Huang. 1977. Flagellar mutants of Chlamydomonas: studies of radial spoke-defective strains by dikaryon and revertant analysis. *Proc Natl Acad Sci U S A*. 74:3456-3460.
- McNally, K.P., O.A. Bazirgan, and F.J. McNally. 2000. Two domains of p80 katanin regulate microtubule severing and spindle pole targeting by p60 katanin. *J Cell Sci*. 113 ( Pt 9):1623-1633.
- Merchant, S.S., S.E. Prochnik, O. Vallon, E.H. Harris, S.J. Karpowicz, G.B. Witman, A. Terry, A. Salamov, L.K. Fritz-Laylin, L. Marechal-Drouard, W.F. Marshall, L.H. Qu, D.R. Nelson, A.A. Sanderfoot, M.H. Spalding, V.V. Kapitonov, Q. Ren, P. Ferris, E. Lindquist, H. Shapiro, S.M. Lucas, J. Grimwood, J. Schmutz, P. Cardol, H. Cerutti, G. Chanfreau, C.L. Chen, V. Cognat, M.T. Croft, R. Dent, S. Dutcher, E. Fernandez, H. Fukuzawa, D. Gonzalez-Ballester, D. Gonzalez-Halphen, A. Hallmann, M. Hanikenne, M. Hippler, W. Inwood, K. Jabbari, M. Kalanon, R. Kuras, P.A. Lefebvre, S.D. Lemaire, A.V. Lobanov, M. Lohr, A. Manuell, I. Meier,

- L. Mets, M. Mittag, T. Mittelmeier, J.V. Moroney, J. Moseley, C. Napoli, A.M. Nedelcu, K. Niyogi, S.V. Novoselov, I.T. Paulsen, G. Pazour, S. Purton, J.P. Ral, D.M. Riano-Pachon, W. Riekhof, L. Rymarquis, M. Schroda, D. Stern, J. Umen, R. Willows, N. Wilson, S.L. Zimmer, J. Allmer, J. Balk, K. Bisova, C.J. Chen, M. Elias, K. Gendler, C. Hauser, M.R. Lamb, H. Ledford, J.C. Long, J. Minagawa, M.D. Page, J. Pan, W. Pootakham, S. Roje, A. Rose, E. Stahlberg, A.M. Terauchi, P. Yang, S. Ball, C. Bowler, C.L. Dieckmann, V.N. Gladyshev, P. Green, R. Jorgensen, S. Mayfield, B. Mueller-Roeber, S. Rajamani, R.T. Sayre, P. Brokstein, et al. 2007. The *Chlamydomonas* genome reveals the evolution of key animal and plant functions. *Science*. 318:245-250.
- Minotti, A.M., S.B. Barlow, and F. Cabral. 1991. Resistance to antimetabolic drugs in Chinese hamster ovary cells correlates with changes in the level of polymerized tubulin. *J Biol Chem*. 266:3987-3994.
- Okreglak, V., and D.G. Drubin. 2010. Loss of Aip1 reveals a role in maintaining the actin monomer pool and an in vivo oligomer assembly pathway. *J Cell Biol*. 188:769-777.
- Pazour, G.J., N. Agrin, J. Leszyk, and G.B. Witman. 2005. Proteomic analysis of a eukaryotic cilium. *J Cell Biol*. 170:103-113.
- Piao, T., M. Luo, L. Wang, Y. Guo, D. Li, P. Li, W.J. Snell, and J. Pan. 2009. A microtubule depolymerizing kinesin functions during both flagellar disassembly and flagellar assembly in *Chlamydomonas*. *Proc Natl Acad Sci U S A*. 106:4713-4718.

- Picone, R., X. Ren, K.D. Ivanovitch, J.D. Clarke, R.A. McKendry, and B. Baum. 2010. A polarised population of dynamic microtubules mediates homeostatic length control in animal cells. *PLoS Biol.* 8:e1000542.
- Schuck, S., W.A. Prinz, K.S. Thorn, C. Voss, and P. Walter. 2009. Membrane expansion alleviates endoplasmic reticulum stress independently of the unfolded protein response. *J Cell Biol.* 187:525-536.
- Sharma, N., J. Bryant, D. Wloga, R. Donaldson, R.C. Davis, M. Jerka-Dziadosz, and J. Gaertig. 2007. Katanin regulates dynamics of microtubules and biogenesis of motile cilia. *J Cell Biol.* 178:1065-1079.
- Sharma, N., Z.A. Kosan, J.E. Stallworth, N.F. Berbari, and B.K. Yoder. 2011. Soluble levels of cytosolic tubulin regulate ciliary length control. *Mol Biol Cell.* 22:806-816.
- Srayko, M., D.W. Buster, O.A. Bazirgan, F.J. McNally, and P.E. Mains. 2000. MEI-1/MEI-2 katanin-like microtubule severing activity is required for *Caenorhabditis elegans* meiosis. *Genes Dev.* 14:1072-1084.
- Srayko, M., T. O'Toole E, A.A. Hyman, and T. Muller-Reichert. 2006. Katanin disrupts the microtubule lattice and increases polymer number in *C. elegans* meiosis. *Curr Biol.* 16:1944-1949.
- Warr, J.R., A. McVittie, S.J. Randall, and J.M. Hopkins. 1966. Genetic control of flagellar structure in *Chlamydomonas reinhardtii*. *Genetical Research.* 7:335-351.
- Yu, W., J.M. Solowska, L. Qiang, A. Karabay, D. Baird, and P.W. Baas. 2005. Regulation of microtubule severing by katanin subunits during neuronal development. *J Neurosci.* 25:5573-5583.

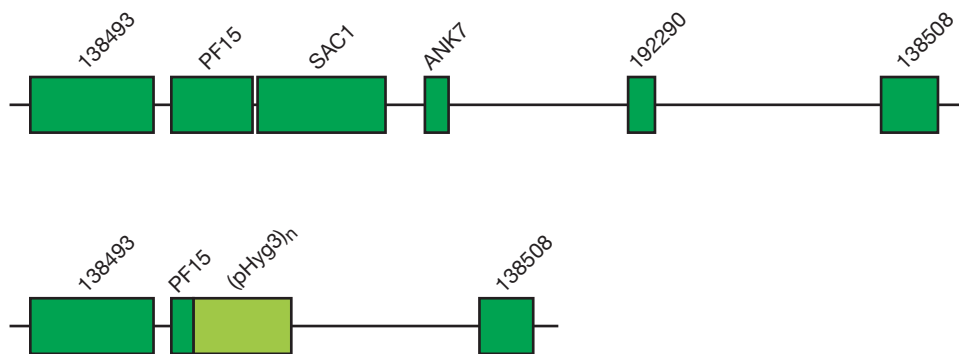
## FIGURES & TABLES

### Figure 1. Genomic region of insertion in mutant 1464

- (A) The relevant region of Linkage Group III is shown for a wild type strain (top) and mutant 1464 (bottom). An unknown number of tandem insertions of the pHyg3 cassette and a deletion of ~25kb are linked to the phenotype in mutant 1464.
- (B) Architecture of the *PF15* gene, with the region deleted in mutant 1464 as indicated.



**A**



**B**

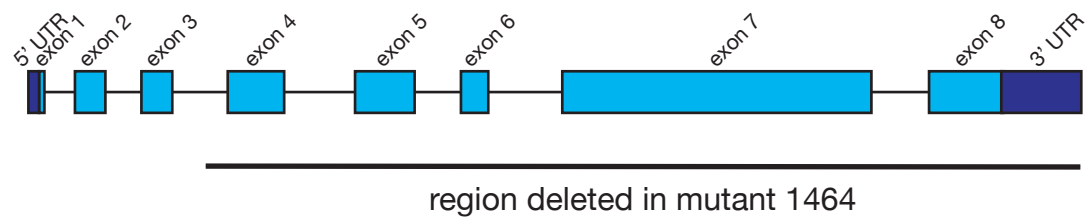


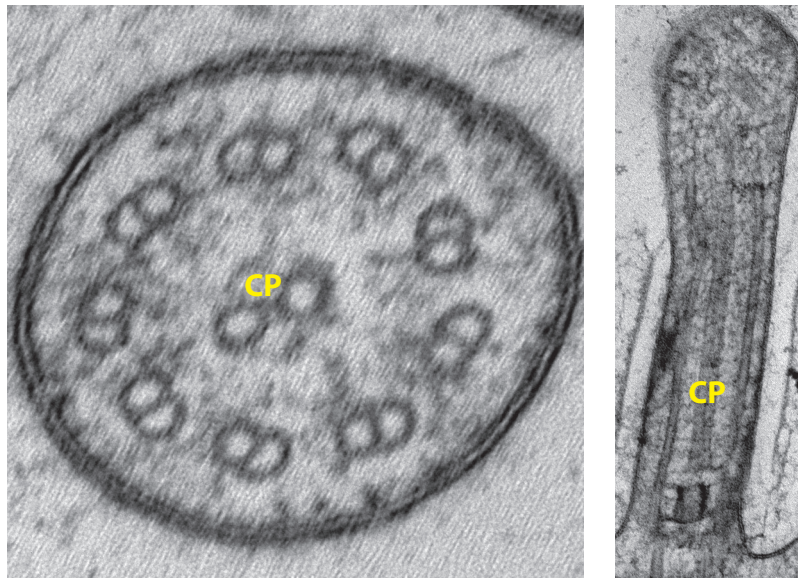
**Figure 2. Electron micrographs of axonemes**

(A) Transverse and longitudinal sections of wild type cc-125 *Chlamydomonas* flagella.

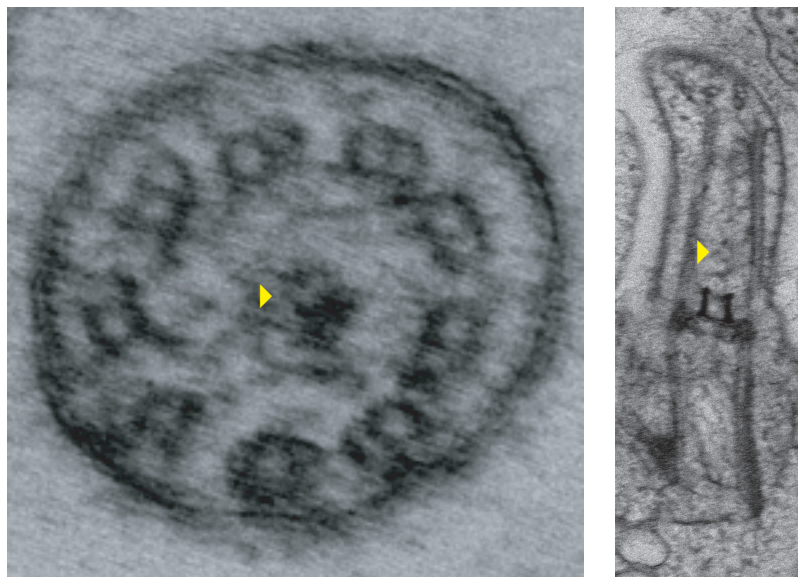
“CP” indicates the central pair of microtubules.

(B) Transverse and longitudinal sections of mutant 1464 flagella. Arrowheads indicate the presence of electron-dense material in place of the central pair.

**A**



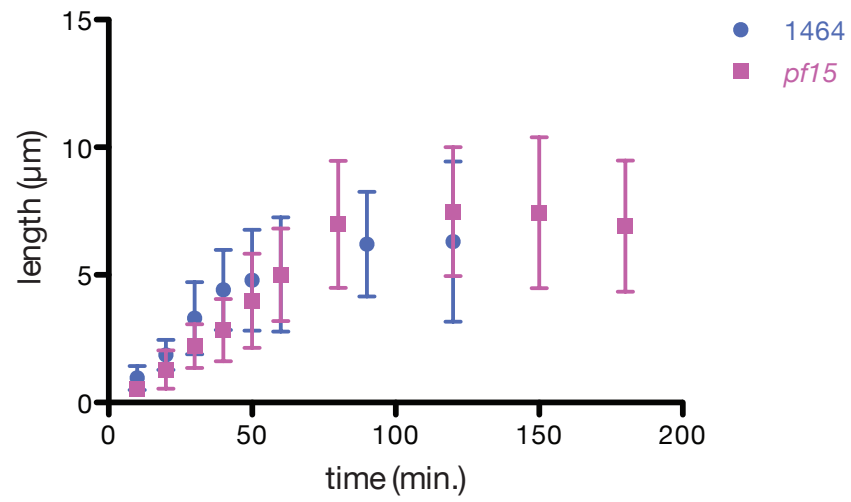
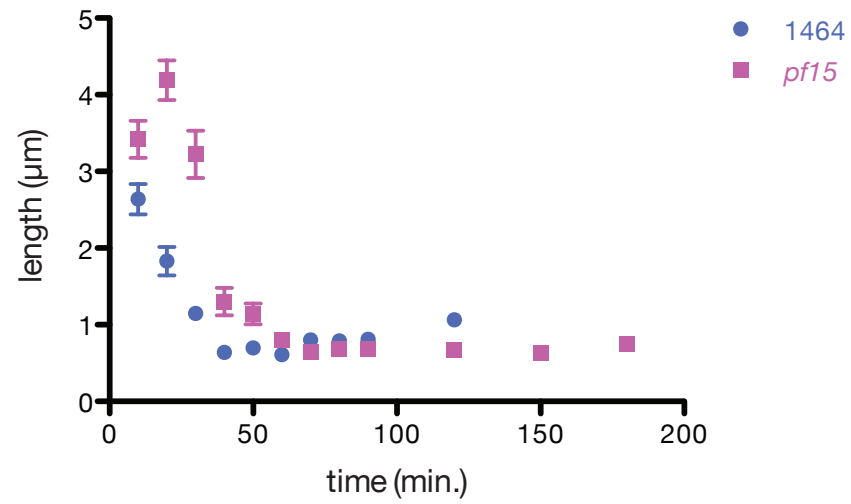
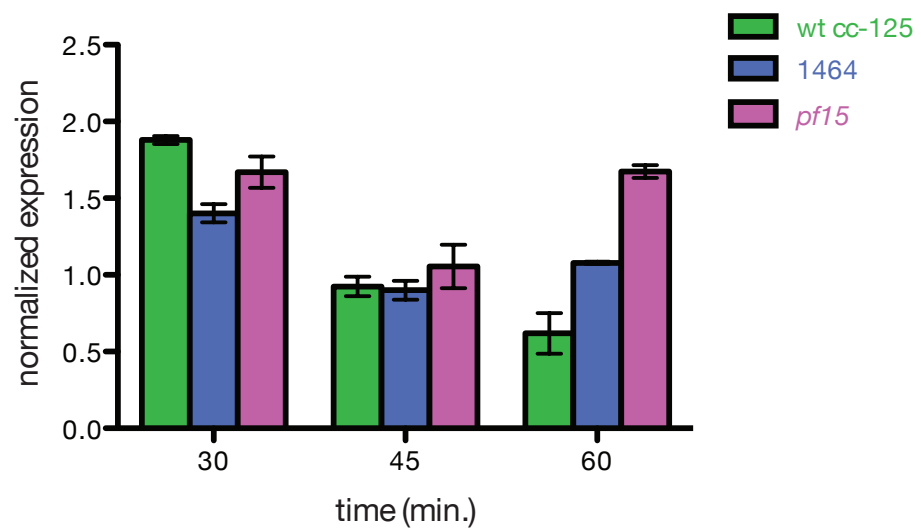
**B**



**Figure 3. Mutant 1464 and *pf15* have nearly identical phenotypes**

Flagellar regeneration, precursor pool dynamics, and radial spoke protein 3 (*RSP3*) gene expression were assayed as described in Chapter 2. Results for wild type strain cc-125 and mutant 1464 are reproduced for reference.

- (A) Both *pf15* and mutant 1464 exhibit similar flagellar regeneration kinetics, with minimal growth after approximately 60 minutes.
- (B) Although the two strains differ slightly in kinetics of pool depletion, neither strain regenerates the pool of flagellar precursors within the expected time frame.
- (C) Both strains have similar levels of *RSP3* induction, however they differ with respect to the duration of induction. There is a statistically significant difference in expression level after 60 minutes of regeneration ( $p < .0001$ ).

**A****B****C**

**Figure 4. Treatment with oryzalin**

TAP agar plates were prepared with 2µm, 20µm, or 40µm oryzalin and control plates with .5% DMSO. Cells were streaked onto duplicate plates and allowed to grow under continuous light for one week. Beginning with the upper left quadrant and continuing clockwise, the strains were streaked as follows: strain 1464, *pf15*, *cw10* (a cell wall deficient mutant), and wild type strain cc-125.

DMSO  
control

oryzalin

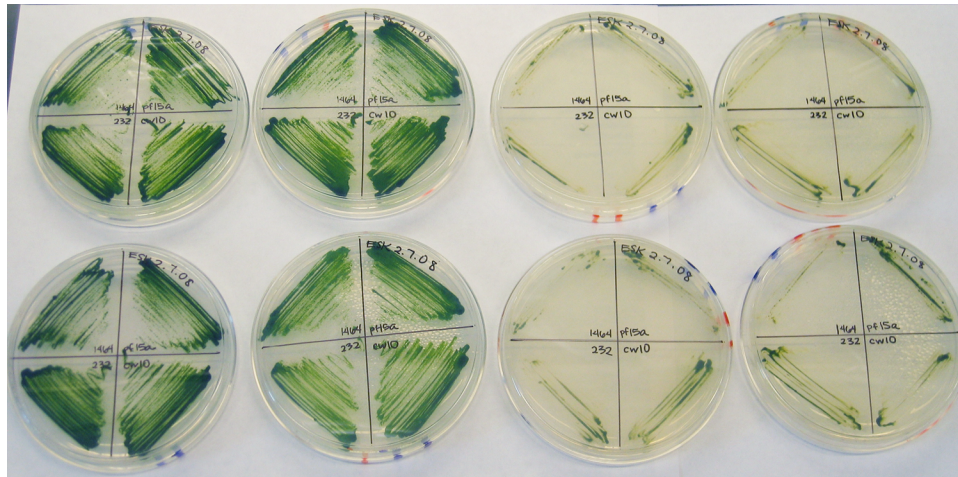


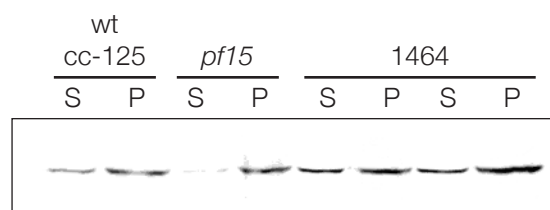
### **Figure 5. Quantification of soluble and polymer tubulin content**

Cells were collected, deflagellated, lysed and centrifuged to separate soluble tubulin from insoluble polymerized tubulin. Flagella were discarded to avoid any differences in polymer content that might be due to variable length flagella.

- (A) Fractionated lysates were separated by SDS-PAGE, transferred to nitrocellulose membranes, and quantified. S and P denote supernatant and pellet, respectively.
- (B) The tubulin polymer ratio was calculated by dividing the amount of polymerized tubulin by the amount of soluble tubulin in the accompanying sample. Although mutant 1464 and *pf15* appeared to have a modestly higher tubulin polymer ratio, the difference was not statistically significant.



**A**



**B**

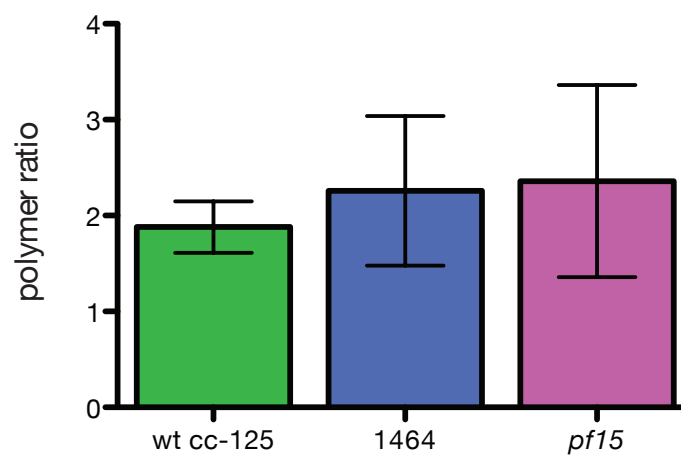


**Table 1. Flanking sequences identified in insertional *shf* mutants**

strain	class	genomic region
1464	III	chromosome 3: PF15 katanin p80
3584	III	chromosome 3: hypothetical TBP-associated factor chromosome 16: predicted heme peroxidase
4580	III	chromosome 13: predicted transcription factor TFIID chromosome 5: uncharacterized protein ID 155845
9111	II	scaffold 29; poorly characterized

## Chapter 4: Summary & Perspective

The goal of my research has been to probe the mechanisms that regulate flagellar length by using mutants with abnormally short flagella and attempting to understand what causes the short flagella phenotype. When I began this work, three short flagella (*shf*) mutants had been described in the literature, but the corresponding genes were not known, and it was not known whether these mutations affected length via similar mechanisms. At the same time, while it was known that flagellar precursor pool production was important for determining flagellar length, little was known about the pathways regulating pool synthesis. It was my hope, in starting this project, that in the course of analyzing *shf* mutants, I might uncover genes important for flagellar precursor pool regeneration or maintenance.

Rather than pursue the existing *shf* mutants, which were point mutations and therefore difficult to clone using existing methods, I chose instead to begin by extensively characterizing the phenotypes of a collection of twenty novel insertional mutants with short flagella, classifying them by features of their flagellar length distributions and utilizing these data to inform further experiments to elucidate the mechanisms giving rise to flagellar length defects. My strategy focused on analysis of flagellar regeneration kinetics, which has long been a useful approach to the understanding of mechanisms of flagellar assembly and its control. In addition to performing the classic experiment in which the lengths of regenerating flagella are measured at discrete time points, I utilized the protein synthesis inhibitor cycloheximide and dual deflagellation experiments to assess the pool of flagellar precursors and employed quantitative RT-PCR to measure gene expression during regeneration.

My major findings from this phenotypic analysis of the *shf* mutant collection include the identification of the first known mutants with defects in the maintenance, accessibility, or regeneration of the flagellar precursor pool. I have also identified new mutants with differences in gene expression during flagellar regeneration, a particularly exciting result because nothing is yet known about factors controlling expression of flagellar genes in *Chlamydomonas*. Identification of the genetic lesion in mutant 784, which fails to induce flagellar gene expression during regeneration and has a defect in regenerating the precursor pool, may yield significant insight into this process.

These analyses focused my interest on mutants that affected pool regeneration. By cloning one of the new *SHF* genes that had an apparent defect in pool synthesis, I uncovered a previously unsuspected role for katanin in flagellar length control. Although we do not yet understand how katanin exerts its effects on flagella at a biochemical level, we have developed a model in which katanin regulates the pool of soluble tubulin available for incorporation into the flagellar axoneme such that decreased katanin activity would lead to less free tubulin and thus shorter flagella. Planned experiments to test this model include katanin overexpression and analysis of existing *Chlamydomonas* strains with hyperstabilized microtubules. My survey of insertional mutants has laid the foundation for many experiments in the future which will further our understanding of flagellar assembly, regeneration, and length control. I have identified flanking sequence in four other insertional mutants, and it will be of great interest to identify the molecular defects underlying the phenotypes we have characterized.

My approach has focused on flagellar length control in populations, but it will be very interesting to investigate this question on a single cell basis. Each of the Class III mutant strains is capable of growing full-length flagella, but only a small percentage of cells in the population do so. Given this heterogeneity, it would be informative to compare and contrast the results of single cell regeneration experiments conducted on cells within a particular strain to address the question of cellular memory. Future analysis of length control in individual cells will be facilitated by new microfluidic methods currently being developed in the lab.


While there is still much to learn about flagellar length control and its repercussions for organelle size regulation as well as human health and disease, the field of organelle size control has been expanding recently. Imaging and computational techniques have advanced significantly, enabling quantitative analysis of organelles with more intricate three-dimensional morphology, such as the endoplasmic reticulum, mitochondria, and vacuoles. It is gratifying to reflect on how much progress has been made toward understanding the regulation of organelle size and establishment of cell architecture, and humbling to think about how much we still don't understand about these fundamental yet complex issues.

**Publishing Agreement**

*It is the policy of the University to encourage the distribution of all theses, dissertations, and manuscripts. Copies of all UCSF theses, dissertations, and manuscripts will be routed to the library via the Graduate Division. The library will make all theses, dissertations, and manuscripts accessible to the public and will preserve these to the best of their abilities, in perpetuity.*

***Please sign the following statement:***

*I hereby grant permission to the Graduate Division of the University of California, San Francisco to release copies of my thesis, dissertation, or manuscript to the Campus Library to provide access and preservation, in whole or in part, in perpetuity.*

  
\_\_\_\_\_  
Author Signature

24 May 2011  
Date